PERFORMANCE MODELLING OF ELECTRIC THREE-WHEELERS ON INDIAN ROADS AND DEVELOPMENT OF RANGE EXTENSION STRATEGY

THESIS SUBMITTED IN PARTIAL FULFILMENTS OF THE REQUIREMENT FOR THE DEGREE OF MASTER OF ENGINEERING IN AUTOMOBILE ENGINEERING UNDER FACULTY OF ENGINEERING AND TECHNOLOGY

Submitted by

RITTIK DAS

Class Roll No.: 002111204008

Examination Roll No.: M4AUT23002

Registration No.: 160302 of 2021-22

Academic Session: 2021-2023

Under the guidance of

Prof. Achintya Mukhopadhyay

&

Dr. Sourav Sarkar

Department of Mechanical Engineering

Jadavpur University

DEPARTMENT OF MECHANICAL ENGINEERING

JADAVPUR UNIVERSITY

188, RAJA S.C. MULLICK ROAD, KOLKATA - 700 032

2023

DECLARATION OF ORIGINALITY AND COMPLIANCE OF ACADEMIC ETHICS

It is hereby declared that the thesis entitled "**PERFORMANCE MODELLING OF ELECTRIC THREE-WHEELERS ON INDIAN ROADS AND DEVELOPMENT OF RANGE EXTENSION STRATEGY**" contains literature survey and original research work by the undersigned candidate, as a part of his degree of Master of Engineering in Automobile Engineering under the Department of Mechanical Engineering, during academic session 2021-2023.

All information in this document have been obtained and presented in accordance with the academic rules and ethical conduct.

It is also declared that all materials and results, not original to this work have been fully cited and referred throughout this thesis, according to the rules of ethical conduct.

Name:	**RITTIK DAS**
Class Roll Number:	**002111204008**
Examination Roll Number:	**M4AUT23002**
University Registration Number:	**160302** of **2021-22**

Date: / / 2023

_____

(Signature)

RITTIK DAS

Department of Mechanical Engineering

Jadavpur University, Kolkata – 700 032

FACULTY OF ENGINEERING & TECHNOLOGY

DEPARTMENT OF MECHANICAL ENGINEERING

JADAVPUR UNIVERSITY

KOLKATA – 700 032

CERTIFICATE OF RECOMMENDATION

This is to certify that the thesis entitled "**PERFORMANCE MODELLING OF ELECTRIC THREE-WHEELERS ON INDIAN ROADS AND DEVELOPMENT OF RANGE EXTENSION STRATEGY**" is a bona fide work carried out by Mr. Rittik Das under our supervision and guidance in partial fulfilment of the requirements for awarding the degree of Master of Engineering in Automobile Engineering under Department of Mechanical Engineering, Jadavpur University during the academic session 2021-2023.

THESIS SUPERVISOR

Prof. Achintya Mukhopadhyay

Professor

Department of Mechanical Engineering

Jadavpur University, Kolkata

THESIS SUPERVISOR

Dr. Sourav Sarkar

Assistant Professor

Department of Mechanical Engineering

Jadavpur University, Kolkata

Prof. Amit Karmakar

Head of the Department

Department of Mechanical Engineering

Jadavpur University, Kolkata

Prof. Ardhendu Ghoshal

Dean

Faculty Council of Engineering & Technology

Jadavpur University, Kolkata

FACULTY OF ENGINEERING & TECHNOLOGY

DEPARTMENT OF MECHANICAL ENGINEERING

JADAVPUR UNIVERSITY

KOLKATA – 700 032

CERTIFICATE OF APPROVAL

*The foregoing thesis, entitled "**PERFORMANCE MODELLING OF ELECTRIC THREE-WHEELERS ON INDIAN ROADS AND DEVELOPMENT OF RANGE EXTENSION STRATEGY**" is hereby approved as a creditable study in the area of Automobile Engineering carried out and presented by Mr. Rittik Das (Registration No.: 160302 of 2021-22) in a satisfactory manner to warrant its acceptance as a prerequisite to the degree for which it has been submitted. It is notified to be understood that by this approval, the undersigned do not necessarily endorse or approve any statement made, opinion expressed and conclusion drawn therein but approve the thesis only for the purpose for which it has been submitted.*

Committee of final evaluation of thesis:

(Signature of Examiners)

Acknowledgements

I would like to take this opportunity to express my heartfelt gratitude and appreciation to all those who have contributed to the successful completion of my final year thesis. This journey has been a culmination of efforts, guidance, and support from numerous individuals, and I am truly thankful for their invaluable contributions.

First and foremost, I extend my deepest gratitude to my supervisor, Prof. Achintya Mukhopadhyay for his unwavering support, guidance, and mentorship throughout this research endeavour. His expertise, constant encouragement, and insightful feedback have been instrumental in shaping the direction of my work and pushing me to achieve excellence. I am sincerely grateful for his dedication and for providing me with the opportunity to delve into the depths of Mechanical Engineering. I would then like to render my sincere gratitude to Dr. Sourav Sarkar for helping me in finding a research domain right in the beginning and believing in my potential. I am grateful to both of my supervisors for providing me an opportunity to conduct this research work in such an interesting discipline.

I extend my gratitude to all the professors specially Dr. Aranyak Chakravarty, who have shared their knowledge, provided valuable suggestions, and offered technical assistance throughout my thesis work. I am indebted to every faculty and staff of the Department of Mechanical Engineering at Jadavpur University. Their support, guidance, and provision of necessary resources have been crucial in facilitating my research.

I am deeply thankful to my fellow classmates, friends specially Ajit Das and research scholars specially Saumendra Nath Mishra, Joy Mandal, Sudipta Saha, Manish Manna, Arindam Mandal, and Sabyasachi Mondal who have provided a supportive and collaborative atmosphere throughout this journey. Their stimulating discussions, shared experiences, and unwavering encouragement have played a significant role in shaping my ideas and improving the quality of my research. I am grateful for their camaraderie and friendship, which have made this experience more fulfilling and enjoyable.

Lastly, I would like to express my deepest gratitude to my parents for their constant love, understanding, and support. Their belief in my abilities and their unwavering

encouragement have been a tremendous source of strength and motivation. I am truly blessed to have them by my side.

In conclusion, this final year thesis represents the culmination of years of hard work, dedication, and collaboration. I am deeply grateful to all those who have played a part, no matter how big or small, in shaping my research and academic growth. Your support has been invaluable, and I am truly thankful for the privilege of learning from and working with such exceptional individuals.

Rittik Das
Department of Mechanical Engineering
Jadavpur University, Kolkata – 700 032
Date: / / 2023

Abstract

In terms of point-to-point connectivity and convenience, internal combustion engine powered three-wheeler auto rickshaws are the most preferred mode of public transport in India and some other Asian countries for short-distance commuting within a city and its environs. Since three-wheeler auto rickshaws are the most preferred mode of public transport, the number of these commercial passenger vehicles is also increasing day by day as the population increases. In view of the fact that these vehicles have engines, requiring fuel to carry out the combustion process and after combustion, they emit hazardous gases such as CO_2, NOx and much more, which are not only harmful to the environment but also pose a threat to human health. To mitigate the adverse impacts of conventional internal combustion engines, a reliable, modern, and alternative solution is needed. For this reason alone, the automobile sector is transitioning to a new generation of eco-friendly electric vehicles. The electric vehicle revolution in India is being spearheaded by the development of pure electric three-wheeler auto rickshaws, but its popularity is curtailed by factors such as energy storage demand and range extension. This research work attempts to fill this gap by simulating a pure electric three-wheeler auto rickshaw, following Indian driving cycle and modified Indian driving cycle, with all essential parameters to calculate its energy, power, and torque demands as well as the battery pack capacity using Microsoft Excel. An approach is outlined for conserving energy or leveraging the conserved energy to extend the overall range of the vehicle. A detailed comparison has been made between the amount of energy gained through 40% and 50% regenerative braking and energy saved by driving in energy saving mode (following modified Indian driving cycle, where velocity is capped at 20 kmh^{-1}) for the last 25 km, resulting in an increase of 39.29% & 45.30%, and 85.12% & 91.95% in range, respectively.

Keywords: *Electric Vehicles, Pure electric vehicles, driving range extension, three-wheeler auto rickshaw, power saving mode*

Table of Contents

List of Figures

List of Tables

Nomenclature

English Symbols

A	Area (m^2)
a	Acceleration (ms^{-2})
C	Coefficient (dimensionless)
E	Energy (J)
F	Force (N)
g	Gravitational acceleration (ms^{-2})
H	Overall height (mm)
L	Overall length (mm)
M	Mass (kg)
P	Power (W)
R	Regeneration efficiency (dimensionless)
r	Radius (m)
T	Torque (N.m)
t	Time (s)
W	Overall width (mm)

Greek Symbols

η	Efficiency (dimensionless)
ρ	Density of air (kgm^{-3})
υ	Resultant velocity (ms^{-1})
Ψ	Angle of inclination (°)

Subscripts

ad	Aerodynamic drag
f	Frontal
hc	Hill climbing
la	Linear acceleration
m	Motor
rr	Rolling resistance
t	Tractive
w	Wheel
ωa	Rotational acceleration

Acronyms

AC	Alternating Current	GVW	Gross Vehicle Weight
AMT	Automated Manual Transmission	HC	Hydrocarbons
AQI	Air Quality Index	ICE	Internal Combustion Engine
ARAI	Automotive Research Association of India	ICEs	Internal Combustion Engines
BEV	Battery-powered Electric Vehicle	IDC	Indian Driving Cycle
BEVs	Battery-powered Electric Vehicles	IS	Indian Standard
BIS	Bureau of Indian Standards	LFP	Lithium Ferro Phosphate
BLDC	Brushless Direct Current	LPG	Liquefied Petroleum Gas
CFD	Computational Fluid Dynamics	MGT	Micro Gas Turbines
CMVR	Central Motor Vehicles Rules	MIDC	Modified Indian Driving Cycle
CNG	Compressed Natural Gas	MIDCs	Modified Indian Driving Cycles
CO	Carbon monoxide	MoRTH	Ministry of Road Transport and Highways
CO_2	Carbon dioxide	NOx	Nitrogen oxides
DC	Direct Current	PM	Particulate Matter
EDC	European Driving Cycle	PMSM	Permanent-Magnet Synchronous Motor
EUDC	Extra Urban Driving Cycle	RE	Range Extender
EV	Electric Vehicle	REEV	Range Extended Electric Vehicle
EVs	Electric Vehicles	SOC	State of Charge
FI	Fuel Injection	SRM	Switched Reluctance Motor
GDP	Gross Domestic Product	SSB	Solid-State Batteries
GR	Gear Ratio	VRLA	Valve Sealed Lead Acid

Chapter 1

Introduction

1.1 Astonishing impact of internal combustion engines on the automobile sector

The term Internal Combustion Engine (ICE) refers to a heat engine where fuel is burned internally in a combustion chamber, a crucial part of the working fluid flow circuit along with the oxidizer (generally air or oxygen). Combustion is the fundamental chemical process by which energy is released from the air-fuel mixture, partially converting this energy into work. A rotor (in case of Wankel engines), a piston (in case of Piston engines), turbine blades (in case of Gas turbines), or a nozzle (in case of Jet engines) are the primary objects to which the force is applied. The force shifts chemical energy into kinetic energy by moving the part through a distance, using it to move, propel, or power anything connected to the engine.

ICEs have maintained their leading position in the automobile sector since its inception due to advantages such as high power-to-weight ratio, simplicity and ease of manufacture, reasonably efficient and reliable. They can be built with inexpensive materials (such as cast iron, steel, and aluminium), making them cheap to manufacture when mass-produced. Fuels like petrol or diesel provide a lot of energy in a small weight and volume, not only allows for faster refueling, but also good for vehicles that need a long range. Petrol engines have an instantaneous control over power output by throttling the air intake, and much more. Due to the huge dominance of ICEs, the automobile sector now accounts for about 3% of global Gross Domestic Product (GDP), with a larger share in developing nations like India, ranking fourth in the world of automobile manufacturing (contributing 7.1% of overall GDP and 49% of manufacturing GDP) [1]. The only reason this sector has been able to assert and maintain this position as a significant contributor to the global economy is that it has relied heavily on the ICEs since its inception.

1.2 Changing landscape of internal combustion engines: Automobile sector's transition from internal combustion engines to electric vehicles

Fuel is the primary component for carrying out the combustion process in ICEs. Global fuel consumption has increased as a result of the proliferation of vehicles worldwide, leading to a substantial rise in fuel prices. The primary fuels utilized in an ICE such as petrol, diesel, Liquefied Petroleum Gas (LPG), or Compressed Natural Gas (CNG) are generally obtained through fractional distillation from crude oil, a fossil fuel that is found in the earth's crust. These mixtures contain hydrocarbons, formed from diatoms and other organic molecules that have been present for millions of years. The fossil fuel reserves are dwindling day by day, and when examined in detail, the process involved in the natural production of fossils will take a long time and a potential shortage of fossils in the future must be prevented in advance. ICE poses an additional major issue, in terms of emissions. In ideal conditions, carbon would only produce carbon dioxide (CO_2) and water vapour, if burned completely. All products other than CO_2 including particulate matter and gases are often called products of incomplete combustion. Solid particles and liquid droplets can make up particulate matter, with varying levels of composition (might include several organic and inorganic compounds), concentration, and distribution of size. An ICE produces both products of complete and incomplete combustion such as carbon monoxide (CO), nitrogen oxides (NOx), particulate matter (PM), hydrocarbons (HC), and much more. These emissions are not only harmful to the environment but also pose various health risks for humans. The daily rise in the number of vehicles globally has led to an unprecedented surge in pollution levels affecting the whole world.

Alternative fuels can address these two primary issues with ICEs, by conserving petroleum and reducing emissions, but they do have some drawbacks. Unlike fuels extracted from fossils (i.e., fuels from non-renewable resources), alternative fuels are produced from renewable raw materials. As a result, its production and use could be sustained indefinitely. However, combustion of alternative fuels can reduce carbon footprint but NOx emissions that threaten human well-being and the environment

cannot be reduced. This requires a reliable, modern and alternative solution, and it is only for these reasons that the automobile sector is moving towards a generation of eco-friendly Electric Vehicles (EVs) as they are able to counteract the negative effects of conventional ICEs.

The fundamental building blocks of an Electric Vehicle (EV) are electric motor, battery pack, gearbox, power controller, Direct Current (DC)-DC converter, and battery charger. The main feature of an EV that differentiates it from conventional vehicles, is the electric motor, which helps transform electrical energy into kinetic energy, enabling the wheels to rotate. The regenerative braking mechanism is an essential element of an electric motor and reduces the vehicle's velocity by converting the kinetic energy into alternative forms, saving that amount of energy for future use. The battery pack powers the electric motor in an EV and it functions as a direct current storage system, storing energy electrically. The range of a battery pack increases with an increase in their storage capacity. The design of battery pack plays a crucial role in their longevity and functionality. The transmission of mechanical power from the electric motor to the wheels occurs through the gearbox. EVs do not require a multi-speed gearbox, which is advantageous. The transmission efficiency must be high to prevent power losses. A steady voltage is supplied by the battery pack. However, the demands for different EV components are diverse. A power controller is responsible for regulating the operation of an EV. This assists in managing the flow of electrical energy from the battery pack to the electric motor. The pedal pressed by the driver determines the velocity of the vehicle and the frequency of voltage fluctuations fed to the motor. Additionally, it regulates the torque produced. The DC-DC converter distributes the output power of the battery pack to a desired level and also supplies the voltage required to charge an auxiliary battery. The charger (generally located within the vehicle) or the onboard charger monitors various battery characteristics and regulates the current flowing through the battery, converting Alternating Current (AC) power to DC power from the charging port. Rather than using fossil fuels, EVs charge their battery pack with electricity. The architecture of EV is illustrated in Fig. 1-1.

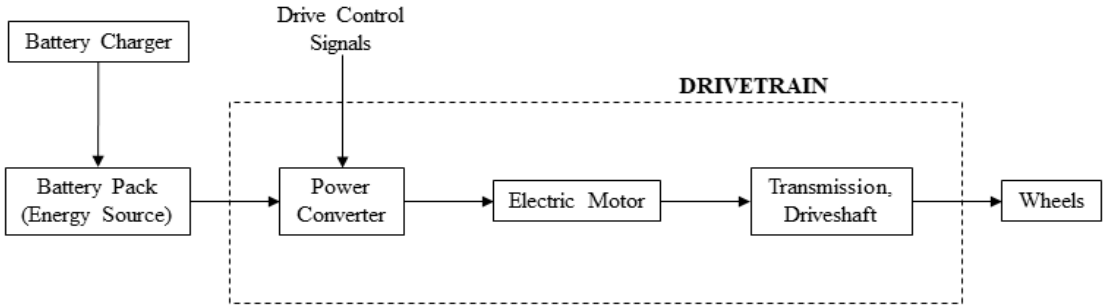

Fig. 1-1: Pure electric powertrain - Architecture of EV

The efficiency of EVs make them a more cost-effective option for charging, which is in stark contrast to the fuel economy of petrol, diesel, LPG or CNG. The main advantage of EVs is that they do not consume any fossil fuels and emit zero emissions, hence use a sustainable form of energy for powering the vehicle.

1.3 Navigating the challenges of implementing the electric vehicle revolution in the automobile sector

The chemical composition and active materials used in an EV battery are used to categorize them. When designing a battery pack for an EV, several factors are taken into consideration, such as its capacity, fast charging capability, and longevity. The battery must be compatible with various operating conditions, including high discharge and charge rates and should match the drive and duty cycles. It must have a heat management and thermal cooling system, and operate at a safe temperature to prevent thermal runaway. Battery pack packaging, reduction of production efficiency (to minimize costs), weight and space constraints must also be considered to ensure that the product is robust and light in weight. Increasing the C-rate of the battery can reduce the charging time, but there are a few caveats. If the C-rate is elevated, the battery will rapidly encounter thermal runaway, rendering it susceptible to fire and explosion. Conversely, to prevent thermal runaway of the battery, its capacity must be compromised, where lower capacity equals shorter range of the battery. Shorter battery range requires frequent charging. This requires charging stations and the infrastructure of EV charging stations is still under development in countries like India. It is nearly impossible to set up gas station type battery charging stations nationwide in a given time frame. The issue of range anxiety is the most significant concern for EV owners,

as they can only use their EVs for shorter ranges than ICEs due to the low energy density of the battery. An additional battery can be used to increase the range of an EV, but the weight of the additional battery will negatively impact range rather than enhancing performance. Correspondingly, an increase in electric motor power will impact its performance, and the additional weight of the vehicle must be transported with more energy. Potential EV buyers in less developed countries have been impeded by the challenge of charging infrastructure and long battery pack durations. Approximately 60–70% of the population of India resides in rural areas, posing a significant challenge for local authorities to install charging stations. Ministry of Power under the Government of India has issued guidelines and standards for EV charging infrastructure on 14th December 2018, revised on 1st October 2019. A draft resolution was made public on 8th June 2020. These guidelines imply that a minimum of one charging station will be present in a 3 km by 3 km mesh area within the city, spread out over 25 km on either side of highways, and that in every 100 km, there will be a minimum of one fast charging station on each side of the highways suitable for long-range electric vehicles such as buses, trucks, etc [2].

Table 1-1: EV chargers as provided under Para 3.1 (vi) of the guidelines and standards issued by Ministry of Power, Government of India [2]

Charger Type	Sl. No.	Charger Connectors	Rated Output Voltage (V)	No. of Connector guns	Charging vehicle type
Fast	1	Combined Charging System (min 50 kW)	200–750 V or higher	1 CG	4W
	2	CHArgedeMOve (min 50 kW)	200–500 V or higher	1 CG	4W
	3	Type-2 AC (min 22 kW)	380–415 V	1 CG	4W, 3W, 2W
Slow / Moderate	4	Bharat DC-001 (15 kW)	48 V	1 CG	4W, 3W, 2W
	5	Bharat DC-001 (15 kW)	72 V or higher	1 CG	4W
	6	Bharat AC-001 (10 kW)	230 V	3 CG of 3.3 kW each	4W, 3W, 2W

The automobile sector encounters significant impediments in leading the industrial revolution, including the issues related to battery charging time, battery range, and battery charging site conditions.

1.4 A comprehensive overview of pure electric three-wheelers

The Air Quality Index (AQI) in many large cities of India is extremely poor as a result of the harmful gas emissions caused by automobiles. India's NITI Aayog has proposed a transition of ICEs into EVs by 2030 to combat the country's persistent environmental pollution problems, which is among the most polluted countries globally, leading to 37% reduction in CO_2 emissions and 64% reduction in energy demand [3]. Contrast to ICEs, EVs are more eco-friendly and energy efficient, emitting no harmful gases while driving. They have fewer moving and reciprocating parts, resulting in less vibration providing zero noise pollution. To address the difficulties the automobile sector currently experiencing with the adoption of EVs, researchers are conducting research on different category of vehicles. While research into EVs has exploded recently, little attention has been given to three-wheelers. In terms of point-to-point connectivity and convenience, three-wheelers are the most preferred mode of public transport in India for short distance commuting within a city and its environs. Prior to the development of e-rickshaws or electric rickshaws, the only other three-wheeler passenger vehicle on the market was an auto rickshaw. E-rickshaws, as illustrated in Fig. 1-2, have been gaining popularity in most parts of the world since 2008 and in India since 2011. E-rickshaws is the best alternative to petrol, diesel, LPG, or CNG powered auto rickshaws as they are battery powered. Unlike auto rickshaws, e-rickshaws do not discharge hazardous gases and therefore do not commit to increased air pollution. The batteries used for the operation of e-rickshaws can be effectively recycled, solving the problem of battery disposal. The batteries can be easily recharged at home or anywhere where sufficient voltage is available. They do not cause noise pollution as they do not produce any noise and because of this, the passengers can have a smooth and comfortable ride. E-rickshaws provide livelihoods for both ordinary people and the illiterate, and without investing a lot of money, drivers can earn a good income. They pose fewer risks than other fuel powered vehicles. They do not have any engine or gearbox, which reduces

the maintenance burden. The motor used in these e-rickshaws is generally smaller and the battery is placed underneath. Therefore, maintaining it is much easier, but it has some major drawbacks. E-rickshaws are generally slower and run at a velocity of around 30-35 kmh^{-1}, meaning they cannot match the speed of other vehicles. In case of an emergency, this is not a preferred mode of transportation. They may overturn because they are lighter in weight and therefore can hardly compete with heavier vehicles. One of the biggest drawbacks of an e-rickshaw is the battery issue and most of the batteries in use are lead acid batteries. The current design of e-rickshaws takes up a lot of space which lead to traffic congestion.

These major drawbacks of the e-rickshaws make it necessary to convert the competing auto rickshaws, as illustrated in Fig. 1-3, into pure EVs, using Li-ion battery pack and this generates a great deal of interest, requiring a thorough analysis of the various factors involved in its design and development in order to bring forward new and efficient technologies. The EV revolution in India is being spearheaded by the development of electric auto rickshaws, but their popularity is curtailed by factors like energy conservation and range extension.

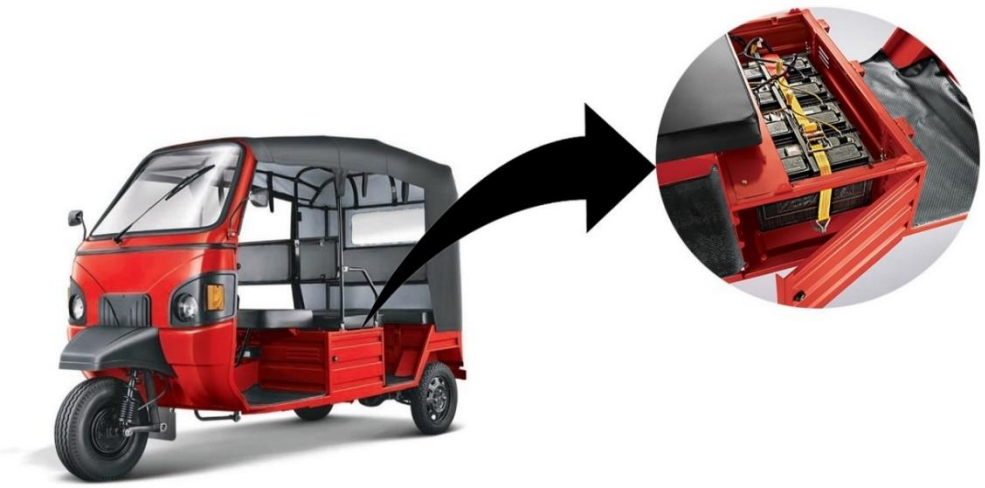

Fig. 1-2: E-rickshaw

If the two limiting factors can be overcome, the pressing environmental problems will be solved through significant reductions in air and noise pollution. Pure electric auto rickshaws will offer a sustainable solution to rising fuel costs, economically benefitting drivers and reducing the country's dependence on fossil fuels. In addition, switching to

pure electric can improve the livelihoods of auto rickshaw drivers by reducing operating and maintenance costs, thereby increasing their income. Overall, the conversion aligns with India's commitment to cleaner transport and promotes a greener and more sustainable urban transport ecosystem.

Fig. 1-3: Auto rickshaw

1.5 Literature Review

The range extension of EVs is one of the most popular and discussed topics in the automobile sector. A lot of research work has been done on various types of EVs, including hybrid electric, fully electric or pure electric, plug-in electric, and many more. In this literature review subsection, some important studies on range extension of EVs have been conducted, which form the basis of this thesis and are presented and discussed briefly. Ribau et al. [4] compared energy efficiencies and CO_2 emissions of four different types of range extenders, concluding that the consumption of energy of Range Extended Electric Vehicle (REEV) will decrease compared to ICE, only if the major distance travelled is spent to urban travel. Bobba and Rajagopal [5] focused on modelling and analysis of hybrid energy storage systems in EVs and studied the intricacies of these systems. They provided insights into optimization strategies and potential benefits by delving deeper into the design and operation of EV hybrid energy storage systems, contributing to the understanding and advancement of energy storage solutions. Marker et al. [6] suggested that driving behaviour has a substantial impact on

the energy consumption of electrified vehicles, stating that the battery size is the most crucial component of EVs. A Battery-powered Electric Vehicle (BEV) with a large capacity battery is less effective than a REEV with a smaller battery. They also stated that the BEV will only cover 50% of the distance (corresponding to 90% of all daily distances) while the REEV will cover 100% of all daily distances, of which 70% is electric at a given range of 50 km. This leads to lower CO_2 emissions than the combined use of Battery-powered Electric Vehicles (BEVs) and conventional cars. Mishra et al. [7] explored the selection of an appropriate propulsion motor and gear ratio for EVs operating on Indian city roads, with a focus on improving the performance of EVs in urban contexts. They developed criteria for motor and gear ratio selection, considering efficiency, power requirements and road conditions, optimized EV design for Indian city driving scenarios, and advanced technologies of sustainable transport. Sreejith and Rajagopal [8] has elaborated on the process of selecting motors and batteries for three-wheeler EVs. By analysing key considerations such as performance optimization and efficiency, they provided valuable insights into the field of EV technology, helped refine design approaches, and suggested possible future research directions. Xian et al. [9] conducted their studies and concluded that the limited energy density of batteries is a problem for EVs, contributing to driver anxiety about range. A Range Extender (RE) is a possible answer to this problem. This paper provides a parametric analysis of how component size affects REEV performance, including battery capacity, battery cost, and RE performance. The study is mainly carried out for the driving cycle on the highway and in the city. Vidhya and Balaji [10] presented the modelling, design and energy supervision of a hybrid energy storage system for a three-wheeler light EV following Indian conditions for driving. In this paper, the effective coupling of a Li-ion battery and an ultracapacitor coupled to an efficient bi-directional converter is described. A design methodology has been discussed related to vehicle modelling, motor rating selection, converter design, Li-ion battery size, and ultracapacitor pack is presented. Tran et al. [11] provided a descriptive overview of the various types of EV range extension technologies, including ICE, free-piston linear generators, fuel cells, Micro Gas Turbines (MGT), and zinc-air batteries, and described definitions, working mechanisms, and some recent developments of each range extension technology. They also compared the different technologies and highlighted their pros and cons. This is also presented to meet future research needs. Navaneeth et al. [12] have highlighted the significant drawbacks of EV compared to ICE since the beginning of the nineteenth

century, such as shorter and longer refuelling times, higher price and lower range. Different battery chemistries have been utilized since the beginning of the nineteenth century. This gives an overview of the main types of batteries used in EVs and shows the benefits of Solid-State Batteries (SSB) over other chemical batteries. Batteries in particular offer liquid-filled Li-ion batteries. The best battery following IDC was discovered. Several factors including energy density, safety, price, cycle life and many more were compared. He also highlighted why lithium based SSB have potential for utilization in EV applications. Mohammed et al. [13] discussed the conversion of a petrol engine auto rickshaw into an electric-powered three-wheeler with an onboard solar charging system, thereby increasing vehicle performance and increasing range. Switching from a conventional ICE to an electric powertrain addresses environmental concerns and reduce emissions. The integration of a solar charging system adds an innovative dimension and allows longer range without depending solely on the electricity grid.

1.6 Present work

It is evident from the available literature that a significant amount of experimentation and work has been done on extending the range of EVs. Many researchers have tried and found many ways to extend the range of EVs, but little attention has been paid to extend the range of pure electric three-wheeler auto rickshaws. It has been found that a considerable amount of research is required to fully understand the possibilities of extending the range of an auto rickshaw. In this present work, the various forces, including the tractive force, acting on the auto rickshaw following IDC were calculated using selected specifications of an auto rickshaw, and on the basis of the total tractive force, the tractive power required to propel the vehicle was calculated. Motor power was calculated using tractive power and motor efficiency, and tractive torque was calculated from tractive force and wheel radius of the vehicle. Finally, the motor energy demand is calculated based on the motor power at different regeneration efficiencies. On this basis, an estimate of the state of charge was carried out to verify the initial range of the vehicle and thus validate the work. After successful validation, the same process was followed, but this time IDC was not followed, but 6 different modified Indian driving cycles with different capping velocities were used to test the range difference. Then the results were obtained and analysed.

1.7 Layout of the thesis

Chapter 1 explores the extraordinary impact of ICEs on the automobile sector, changing landscape of ICEs: automobile sector's transition from ICEs to EVs, the challenges of implementing EV revolution in the automobile sector, and a brief overview of pure electric three-wheelers. Literatures relevant to the problem of interest are reviewed, along with the discussion about the present work. Chapter 2 discusses the specifications of a three-wheeler auto rickshaw. The significance of selected specifications that directly affect vehicle performance in the broader context of vehicle dynamics and load modelling is also discussed. Chapter 3 performs pure EV load modelling and state of charge estimation. Key factors such as the driving cycle, IDC, tractive force, estimation of energy, power and torque, wheel speed, regenerative braking energy, and state of charge estimation are described together with the formulation of the present work. Chapter 4 discusses the results of the present work on extending the range of a pure electric three-wheeler auto rickshaw. Chapter 5 concludes the present work with some important concluding remarks drawn from the study, as well as the scope of future work.

Chapter 2

Vehicle Specifications

This chapter takes a closer look at the specifications of a three-wheeler auto rickshaw and discusses the importance of various parameters that directly affect vehicle performance in the broader context of vehicle dynamics and load modelling. It is possible to enhance the drivability, safety and overall performance of a vehicle by comprehending the significance of these parameters in a specific dynamic scenario in determining its performance.

Table 2-1: Specifications of a three-wheeler auto rickshaw [14, 15]

Performance	
01 Fuel Type	Electric (Pure EV)
02 Gradeability	29% Maximum, 20% Continuous
03 Maximum Power	4.5 kW (Continuous)
04 Maximum Torque	36 Nm
05 Top Speed	45 kmh^{-1}
06 Transmission	2 Speed AMT
Battery	
07 Type	Li-ion - LFP
08 Battery Capacity	8.9 kWh
09 IP67 Packaging	Yes
Charger	
10 Charging Socket Grid Side	3 Pin 16 Amps
11 Charging Time	4 hours 30 minutes < 3 hours – 80%
12 Cable	RCD cable protects from voltage fluctuation
Suspension System	
13 Front	Single shock absorber with spring
14 Rear	Independent trailing arm with helical spring

Braking System	
15 ABS	No
16 Hill Hold Assist	Yes
17 Parking Brake	Yes
18 Regenerative Braking System	Yes
19 Type	Hydraulic drum brake system
Chassis & Weight Distribution	
20 Chassis Type	Monocoque chassis with cabin
21 Seating Capacity	4 persons (including driver)
22 Curb Weight	*472.17 kg
23 Gross Vehicle Weight, *GVW*	732 kg
Dimensions	
24 Overall Length, *L*	2,714 mm
25 Overall Width, *W*	1,350 mm
26 Overall Height, *H*	1,772 mm
27 Rolling Resistance Coefficient, C_{rr}	0.015
28 Air Drag Coefficient, C_{ad}	0.44
29 Frontal Surface Area, A_f	2.09 m^2
Tyres	
30 Type	Radial tubeless
31 Size	120/80-R12

Only a few key specifications of a three-wheeler auto rickshaw have been selected from the table above, which will be further used in load modelling, as outlined in Table 2-2.

Table 2-2: Selected specifications of an auto rickshaw for load modelling

Sl. No.	Parameters	Values
1.	Gross Vehicle Weight, *GVW*	732 kg
2.	Rolling Resistance Coefficient, C_{rr}	0.015
3.	Air Drag Coefficient, C_{ad}	0.44
4.	Frontal Surface Area, A_f	2.09 m^2
5.	Tyres	120/80-R12

2.1 Curb Weight

For an ICE vehicle, the curb weight is the total weight of the vehicle, including the frame or chassis, the engine, and all essential consumables required for operation such as engine oil, coolant, transmission oil, brake fluid, and a full tank of fuel. However, for a pure EV, the curb weight is the total weight of the vehicle, including the frame or chassis, motor, battery pack, and all essential consumables such as transmission oil and brake fluid. The chassis weight of each specific vehicle type would be the same if the chassis is based on the same platform and built on the same architecture. However, the curb weight would be different for each specific vehicle type as unlike ICE vehicles, pure EVs do not have engines and other associated components, but rather a motor and a battery pack. The curb weight and fuel tank capacity of an LPG model is 384 kg and 20.6 l (Water equivalent) respectively [16].

This present work refers to a pure EV and the actual curb weight is unknown and will be needed later to determine various parameters. However, both LPG and pure EV models are known to have the same chassis counterparts. In order to determine the exact curb weight of a pure EV model, the weight of the chassis must first be determined. As mentioned, although the two models share the same chassis counterparts, their chassis weights are also the same. To determine the exact chassis weight of an LPG model, the weight of the engine, the weight of other associated components and the weight of the fuel must be subtracted from the curb weight. To determine the full tank fuel weight, the maximum fuel volume must be multiplied by the density of water and the specific gravity of LPG. The weight of the engine and other associated components such as the Fuel Injection (FI) system, throttle body, fuel tank, fuel pump and exhaust system is estimated at approximately 64 kg (32 kg for the engine + 3 kg for FI system and throttle body + 14 kg for the fuel tank and the fuel pump + 15 kg for the exhaust system). The fuel weight is 11.33 kg (20.6 × 1 × 0.55). The exact weight of the chassis is therefore 308.67 kg (384 kg – 64 kg – 11.33 kg).

Now, to determine the exact curb weight of a pure EV model, the weight of the motor and battery pack must be added to the weight of the chassis. The weight of a compact 5.2 kW Permanent-Magnet Synchronous Motor (PMSM) is 28.5 kg [17]. The weight

of a Lithium Ferro Phosphate (LFP) battery with a capacity of 8.9 kWh is 135 kg [18]. Thus, the curb weight of a pure EV model is *472.17 kg (308.67 kg + 28.5 kg + 135 kg).

2.2 Gross Vehicle Weight

Gross Vehicle Weight (GVW) refers to the total weight of the vehicle, including parked and moving loads, as declared by the competent authority of the country of registration. It includes the weight of the driver and the maximum number of people allowed. In this case, a maximum of 3 people are allowed as passengers in an auto rickshaw, excluding the driver, according to the standards for category L5M vehicles [19]. According to reports, the average weight of Indian men is 65 kg [20]. Based on this, the weight of 3 passengers is 195 kg (65 kg × 3). Adding the weight of the driver gives a weight of 260 kg (195 kg + 65 kg). Therefore, the gross vehicle weight of a pure EV model is 732.17 kg (472.17 kg + 260 kg) ~ 732 kg.

2.3 Rolling Resistance Coefficient

The rolling resistance coefficient is a parameter which characterizes the resistance undergone by the tyres of a vehicle when they roll on a surface. It is a measure of the energy required to overcome the friction between the rolling surface and tyres. It is usually represented as a dimensionless value or a percentage. It depends on diverse factors, including the type and condition of the tyres, the type and condition of road surfaces, and the load supported by the tyres. In general, softer tyres and rough road surfaces tend to have a higher rolling resistance coefficient and require more energy to maintain forward motion. Conversely, harder tyres and smoother road surfaces result in a lower rolling resistance coefficient, which reduces the energy needed to propel the vehicle. The rolling resistance coefficient helps in determining the vehicle's overall energy consumption. A higher rolling resistance coefficient leads to greater energy losses, requiring more energy to propel the vehicle. Therefore, manufacturers and engineers strive to minimize rolling resistance by optimizing tyre design, selecting tyres with low rolling resistance, and developing a smoother road surface.

2.4 Drag Coefficient

The drag coefficient is a dimensionless quantity that represents the resistance experienced by a body as it moves through a fluid, such as air or water, and quantifies an object's aerodynamic efficiency. It is a crucial parameter for understanding and analyzing the aerodynamic properties of a vehicle in interaction with a fluid medium. The drag coefficient depends entirely on the shape, size and surface finish of the object. It is determined experimentally by wind tunnel tests or CFD (Computational Fluid Dynamics) simulations. A lower drag coefficient means that the object encounters less resistance as it moves through the fluid, resulting in improved efficiency and lower energy consumption. On the other hand, a higher drag coefficient indicates greater endurance and higher energy requirement for movement. The drag coefficient is an essential factor in various technical fields. In automotive design, reducing the drag coefficient helps improve energy demand and vehicle performance. Understanding the drag coefficient and its influence on the overall aerodynamic behavior of objects helps engineers and designers to optimize shapes, reduce drag and improve performance. Significant improvements in efficiency, stability, and speed can be achieved by carefully analyzing and adjusting an object's geometry.

2.5 Frontal Area

The frontal area is the vehicle's cross-sectional area seen from the front. The frontal area plays an important role in aerodynamics and directly affects the drag force experienced by the vehicle. It is usually measured in square units such as square meters and is determined by multiplying the width of the object by its height or diameter, depending on its shape. The larger the frontal area, the greater is the resistance encountered by the object when moving through a fluid medium, such as air. This resistance is known as Drag. Therefore, minimizing the frontal area is an important aspect of vehicle design to reduce drag and improve aerodynamic efficiency. Engineers strive to reduce the frontal area of the vehicle by designing streamlined shapes and minimizing protrusions or unnecessary areas. This helps improve energy efficiency, reduce wind noise and improve overall vehicle performance. The frontal area is often used in conjunction with the drag coefficient to calculate the aerodynamic drag experienced by a vehicle. The relationship between frontal area, drag coefficient and

their influence on vehicle performance has been described in Chapter 3 on Pure EV Load Modelling.

2.6 Tyre

Regardless of the type of vehicle, Tyres are considered the most important component as they affect almost all performance factors such as braking, acceleration, handling and comfort. They provide good grip on the surface, preventing slipping and skidding, so they perform well on both dry and wet road conditions. Tyre functions include load bearing capacity, shock absorption while driving, ability to turn left or right, and optimal acceleration and braking. Tyres can be categorized by the tube used (e.g. tube-type and tubeless-type) and their construction (e.g. cross-ply, radial-ply and bias-ply). The size and material of the tyre must be selected to support the vehicle load and to withstand varying loads during rotation.

Currently, tubeless radial-ply tyres are widely used in the automobile industry because they have lower rolling resistance loss, resulting in lower energy consumption, longer tread life due to reduced heat generation, better braking efficiency and greater resistance to punctures and cuts.

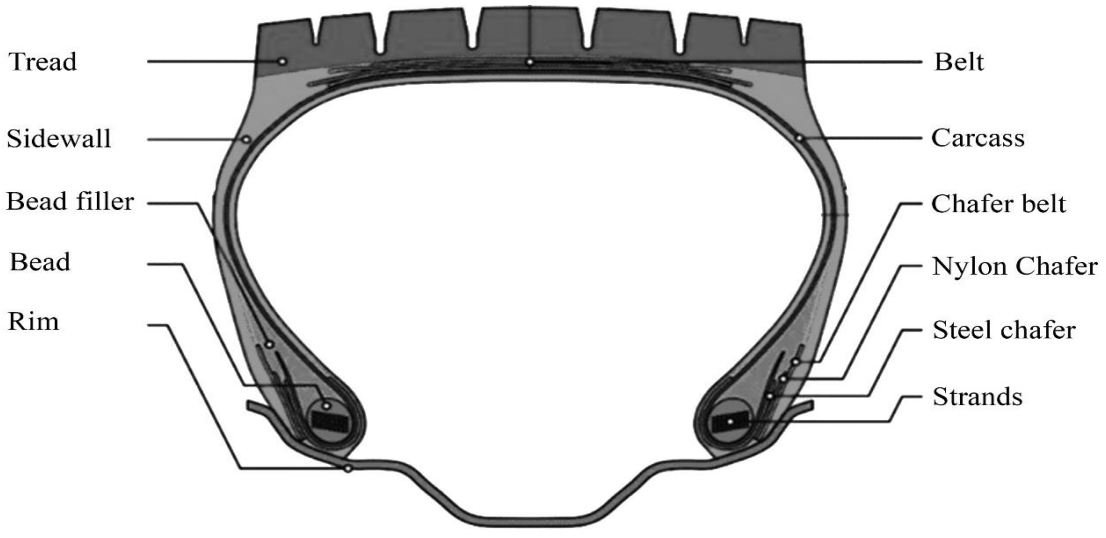

Fig. 2-1: Construction of a radial-ply tyre

Some embossed numbers and letters can be seen, when looked closely at the tyre rubber. These numbers and letters are often referred to as tyre markings. The tyre

markings on the rubber of a tyre are there for a purpose. Firstly, it shows important information such as the size and specification of the tyre and secondly, it proves that the tyre meets the necessary safety standards.

Fig. 2-2: Tyre markings

Tyre markings vary depending on tyre construction. The two most commonly used tyre markings are listed below as examples.

Example 1: 4.00-8, 4PR

This is the simplest tyre marking and is mostly used for bias-ply tyres. The first part, 4.00, is both the tyre width and the tyre sidewall height (in inches). The second part, 8, is the rim diameter (in inches). The last part, 4PR, indicates the ply or load rating. So, a 4.00-8, 4PR tyre will fit on an 8 inches diameter rim, with a width of 4 inches and sidewall height of 4 inches. Therefore, the overall height of the tyre will be 16 inches (8 inches + 4 inches + 4 inches).

Example 2: 120/80-R12 66S

This is the most common tyre marking and is mostly used for radial-ply tyres. The first part, 120, is the tyre width (in millimeters). The second part, 80, is the tyre aspect ratio (tyre width : tyre sidewall height). The third part, R, indicates that the tyre is a radial-ply tyre. The fourth part, 12, is the rim diameter (in inches), the fifth part, 66, indicates the load rating. The last part, S, represents the speed rating. So, a 120/80-R12 66S tyre

will fit on a 12 inches diameter rim, with a width of 120 millimeters and sidewall height of 96 millimeters (80% of 120 millimeters). The overall height of the tyre can be worked out by converting both dimensions to either millimeters or inches, and adding the rim diameter to twice the sidewall height. Therefore, the overall height of the tyre will be 496.8 millimeters (304.8 (12×25.4) millimeters + 96 millimeters + 96 millimeters) or 19.55906 inches (12 inches + 3.77953 (96/25.4) inches + 3.77953 (96/25.4) inches).

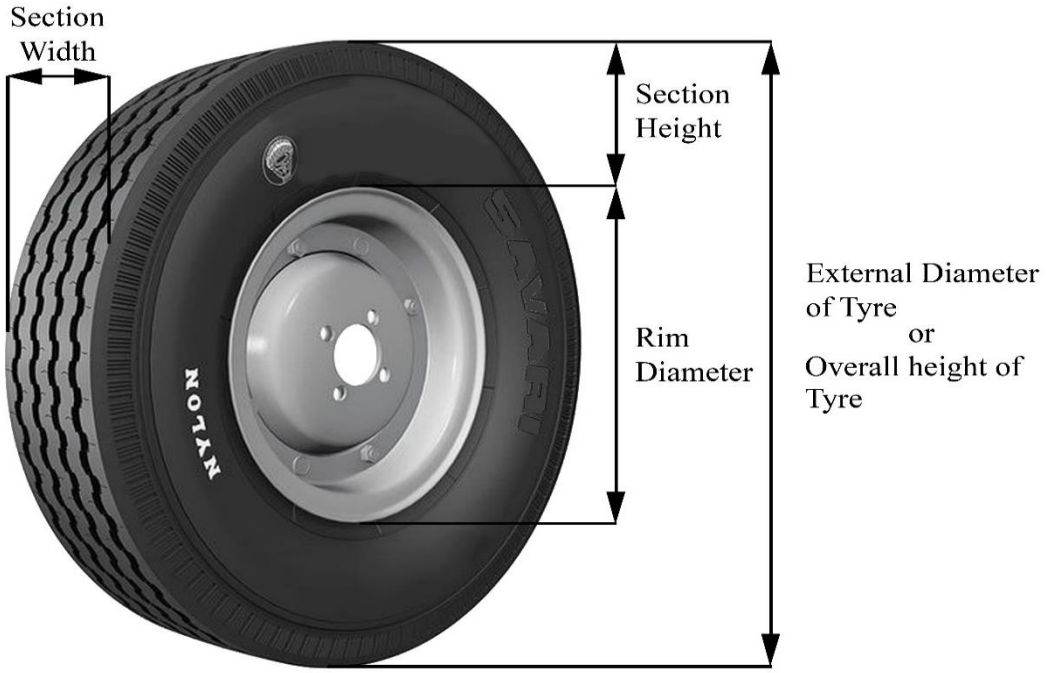

Fig. 2-3: Tyre aspect ratio

2.7 Wheel

Wheel is usually made of a metal or alloy rim, which provides structural strength and houses the tyre. The tyre's bead (inner edge) fits into a groove on the wheel rim, ensuring a secure fit. The wheel, together with the tyre, supports the weight of the vehicle, its occupants, and cargo. The wheel evenly distributes the load across the contact area of the tyre with the road surface, ensuring stability and safe handling. The design of the wheel, such as its width, can affect the shape and footprint of the tyre, affecting traction and grip. The tyre's flexible sidewalls and air-filled construction help absorb shock and provide a cushioning effect. The stiffness and strength of the wheel helps to maintain the structural integrity of the tyre, preventing damage or deformation. The tyre and wheel must be of compatible size. The tyre size, specified by

measurements such as width, aspect ratio and diameter, must match the correct wheel size. Incompatible tyre and wheel sizes can cause improper fitment, impaired handling, and potential safety hazards. The wheel and tyre have a symbolic relationship, where the wheel provides structural support, load distribution and compatibility, while the tyre provides traction, grip, shock absorption and adjustability. Together they are an integral part of the overall performance and safety of the vehicle.

The radius of the wheel plays a significant role in vehicle dynamics, directly influencing several key factors that affects vehicle dynamics. In this present work, the diameter of the wheel is 496.8 millimeters or 19.55906 inches. Therefore, the radius of the wheel is 248.4 millimeters or 9.77953 inches (Diameter of the wheel / 2) and the circumference of the wheel is 1560.406048 millimeters or 61.413379 inches (π × Diameter of the wheel).

Chapter 3

Pure EV Load Modelling

3.1 Driving Cycle

In EV modelling and simulation, driving cycles are used to select and predict the performance of a powertrain system. Driving cycle is a sequence of operating points, representing the vehicle's velocity versus time, and this plot indicates how a vehicle will be driven in a realistic world under various driving conditions. The Automotive Research Association of India (ARAI) has conducted several vivid researches regarding traffic pattern in different Indian cities, establishing the Indian Driving Cycle (IDC), as shown in Fig. 3-1, where a vehicle reaches a maximum velocity of 42 kmh^{-1} in a cycle in accordance with the BIS Code for battery powered vehicles [IS 15886:2010], as well as its various parameters are outlined in Table 3-1 [21]. Any modification to this IDC leads to the formation of Modified Indian Driving Cycle (MIDC). MIDC focuses on the European Driving Cycle (EDC), consisting four repeated cycles of the ECE 15 driving cycle, indicating the urban mode, pursued by the Extra Urban Driving Cycle (EUDC). While realistic, driving cycles do not accurately reflect real-world driving circumstances, for which alternative techniques are applied to acquire the real-time driving cycle [22, 23].

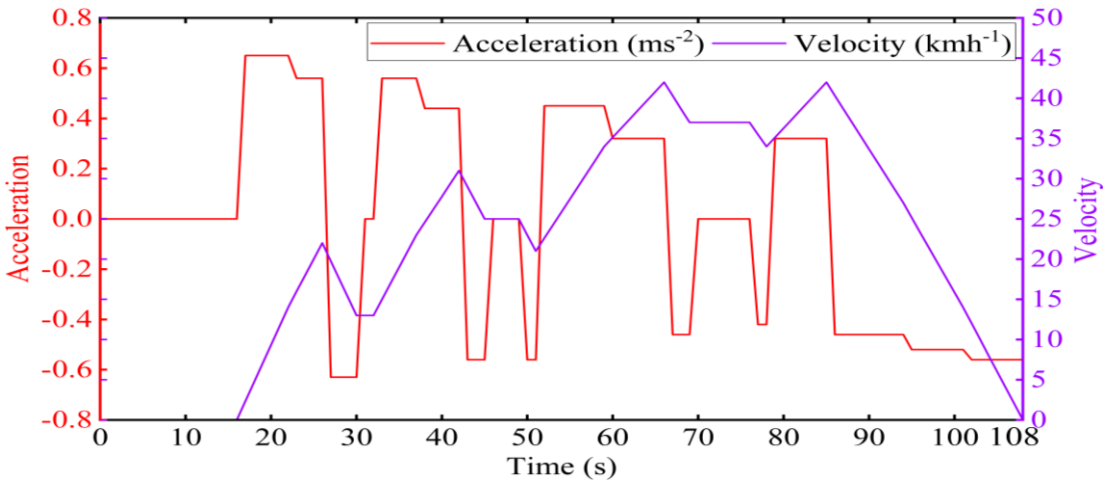

Fig. 3-1: Indian driving cycle (maximum velocity: 42 kmh^{-1})

Table 3-1: Breakdown of Indian driving cycle operations [24]

No. of operations	State	Velocity (kmh^{-1})	Acceleration (ms^{-2})	Duration of each operation (s)	Cumulative Time (s)
01	Idling	0	0	16	16
02	Acceleration	0-14	0.65	6	22
03	Acceleration	14-22	0.56	4	26
04	Deceleration	22-13	-0.63	4	30
05	Steady Speed	13	0	2	32
06	Acceleration	13-23	0.56	5	37
07	Acceleration	23-31	0.44	5	42
08	Deceleration	31-25	-0.56	3	45
09	Steady Speed	25	0	4	49
10	Deceleration	25-21	-0.56	2	51
11	Acceleration	21-34	0.45	8	59
12	Acceleration	34-42	0.32	7	66
13	Deceleration	42-37	-0.46	3	69
14	Steady Speed	37	0	7	76
15	Deceleration	37-34	-0.42	2	78
16	Acceleration	34-42	0.32	7	85
17	Deceleration	42-27	-0.46	9	94
18	Deceleration	27-14	-0.52	7	101
19	Deceleration	14-0	-0.56	7	108

Table 3-2: Summary of an Indian driving cycle (maximum velocity: 42 kmh^{-1})

Idling time (s) in a cycle	16
Total time (s) taken in a cycle	108
Total distance (km) covered in a cycle	0.658
Maximum velocity (kmh^{-1})	42
Average velocity incl. stops (kmh^{-1})	21.93
Maximum acceleration (ms^{-2})	0.65
Maximum deceleration (ms^{-2})	0.63

3.1.1 Indian Driving Cycle (IDC)

An Indian-derived driving cycle has been adopted from the Automotive Research Association of India (ARAI) as this work is conducted for Indian road conditions. According to the selected specifications of a three-wheeler auto rickshaw, reaching a maximum velocity of 45 kmh^{-1} in a cycle, the IDC shown in Fig. 3-2 is taken into account and the data used to represent this figure are outlined in Table 3-3.

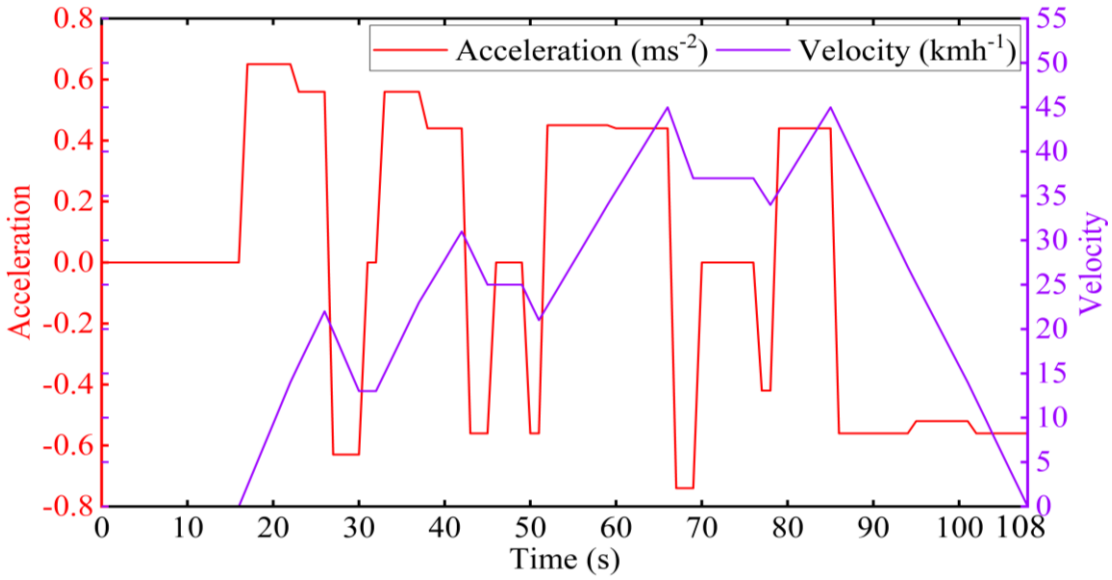

Fig. 3-2: Indian Driving Cycle (IDC)

The idling, steady state, acceleration, and deceleration of a vehicle can be predicted using either Fig. 3-2 or Table 3-3. Table 3-3 can also be used to summarize IDC specifications as shown in Table 3-4. The initial and final velocity at each operation in an IDC are taken from Table 3-3 and converted from kmh^{-1} to ms^{-1} by multiplying the values by the conversion factor of (5/18) or 3.6. By substituting the converted values of the initial and final velocity at each operation into the equation $a = \frac{v-u}{t}$, the acceleration (ms^{-2}) at each operation in an IDC can be calculated, where v is the final velocity (ms^{-1}), u is the initial velocity (ms^{-1}), and t is the time (s). Similarly, by substituting the converted value of the initial velocity, and the calculated value of the acceleration (ms^{-2}) at each operation in an IDC into the equation $S = ut + \frac{1}{2}at^2$, the distance (m) travelled at each operation in an IDC can be calculated, where u is the initial velocity (ms^{-1}), t is the time (s), and a is the acceleration (ms^{-2}). The acceleration and distance distribution for each operation in an IDC are given in Table 3-5.

Table 3-3: Breakdown of selected IDC operations

No. of operations	State	Velocity (kmh^{-1})	Acceleration (ms^{-2})	Duration of each operation (s)	Cumulative Time (s)
01	Idling	0	0	16	16
02	Acceleration	0-14	0.65	6	22
03	Acceleration	14-22	0.56	4	26
04	Deceleration	22-13	-0.63	4	30
05	Steady Speed	13	0	2	32
06	Acceleration	13-23	0.56	5	37
07	Acceleration	23-31	0.44	5	42
08	Deceleration	31-25	-0.56	3	45
09	Steady Speed	25	0	4	49
10	Deceleration	25-21	-0.56	2	51
11	Acceleration	21-34	0.45	8	59
12	Acceleration	34-45	0.44	7	66
13	Deceleration	45-37	-0.74	3	69
14	Steady Speed	37	0	7	76
15	Deceleration	37-34	-0.42	2	78
16	Acceleration	34-45	0.44	7	85
17	Deceleration	45-27	-0.56	9	94
18	Deceleration	27-14	-0.52	7	101
19	Deceleration	14-0	-0.56	7	108

Table 3-4: Selected IDC specification

Sl. No.	Particulars	Time (s)	Percentage
1	Idling	16	14.81 %
2	Steady state points	13	12.04 %
3	Accelerating points	42	38.89 %
4	Decelerating points	37	34.26 %

Table 3-5: Velocity and Distance distribution in an IDC

No. of operations	Duration of each operation (s)	Velocity (ms^{-1})		Acceleration (ms^{-2})	Distance (m)
		Initial	Final		
1	16	0		0	0
2	6	0	3.888888889	0.65	11.7
3	4	3.888888889	6.111111111	0.56	20.03555556
4	4	6.111111111	3.611111111	-0.63	19.40444444
5	2	3.611111111		0	7.222222222
6	5	3.611111111	6.388888889	0.56	25.05555556
7	5	6.388888889	8.611111111	0.44	37.44444444
8	3	8.611111111	6.944444444	-0.56	23.31333333
9	4	6.944444444		0	27.77777778
10	2	6.944444444	5.833333333	-0.56	12.76888889
11	8	5.833333333	9.444444444	0.45	61.06666667
12	7	9.444444444	12.5	0.44	76.89111111
13	3	12.5	10.27777778	-0.74	34.17
14	7	10.27777778		0	71.94444444
15	2	10.27777778	9.444444444	-0.42	19.71555556
16	7	9.444444444	12.5	0.44	76.89111111
17	9	12.5	7.5	-0.56	89.82
18	7	7.5	3.888888889	-0.52	39.76
19	7	3.888888889	0	-0.56	13.50222222

From the above tables, total idling time, total time taken to travel the distance, total distance travelled by the vehicle, maximum velocity, average velocity including stops, maximum acceleration, and maximum deceleration achieved by the vehicle in an IDC can be concluded. All of these factors and their values are summerized in Table 3-6.

Table 3-6: Summary of an IDC

Idling time (s) in a cycle	16
Total time (s) taken in a cycle	108
Total distance (km) travelled in a cycle	0.668
Maximum velocity (kmh^{-1})	45
Average velocity incl. stops (kmh^{-1})	22.29
Maximum acceleration (ms^{-2})	0.65
Maximum deceleration (ms^{-2})	0.74

3.2 Tractive Force

The various forces acting on a vehicle and preventing it from moving forward determine the energy, power, and torque demands of that vehicle. The three-wheeler auto rickshaw is modelled as a road load, and various longitudinal forces acting on it are determined from Newton's second law of motion as illustrated in Fig. 3-3 [5].

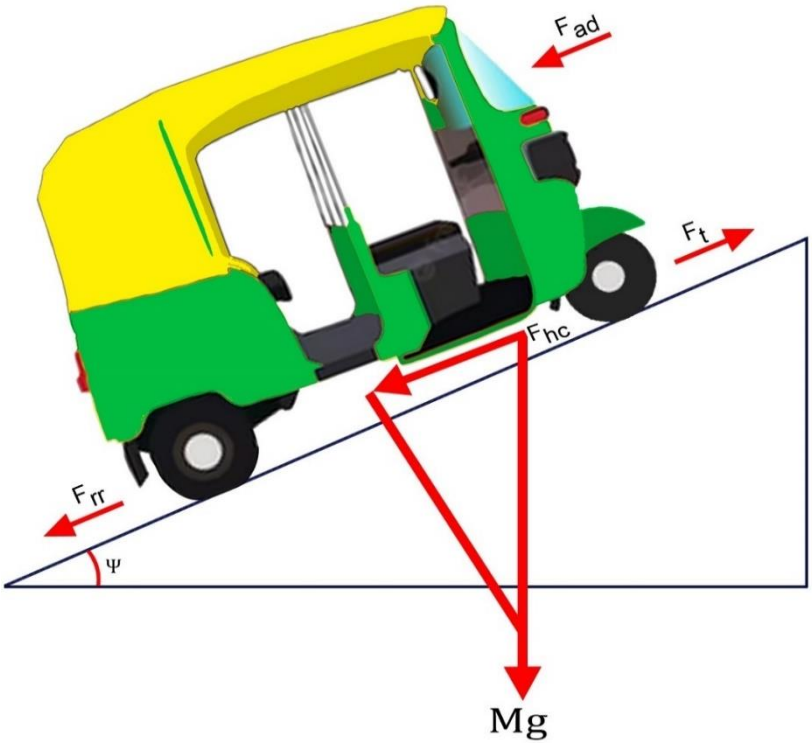

Fig. 3-3: Forces acting on a three-wheeler auto rickshaw during uphill drive

Tractive or traction force, F_t, is the force required to overcome drag forces and move the vehicle forward, and is represented by the equation:

$$\boldsymbol{F_t = F_{rr} + F_{ad} + F_{hc} + F_{la} + F_{\omega a}} \quad (3.1)$$

Where,

F_{rr} = Rolling resistance force

F_{ad} = Aerodynamic drag or drag force

F_{hc} = Hill climbing force or gradient force

F_{la} = Linear acceleration force

$F_{\omega a}$ = Rotational acceleration force

From Eq. (3.1), it is evident that the main force needed to propel the vehicle is the tractive force or the traction force, comprising of five other forces. Namely, Rolling Resistance Force (F_{rr}), Aerodynamic Drag or Drag Force (F_{ad}), Hill Climbing force or Gradient Force (F_{hc}), Linear Acceleration Force (F_{la}) and Rotational Acceleration Force ($F_{\omega a}$).

3.2.1 Rolling Resistance Force

When a wheel or tyre rolls on a surface, rolling resistance force opposes the motion of the wheel or tyre, generally caused by the deformation of the wheel or tyre and the adhesion between the wheel and the surface. The vehicle's ability to move depends on this rolling resistance force, but if it rises above a certain point, the vehicle's energy consumption will also rise.

The equation for rolling resistance force (F_{rr}) is:

$$\boldsymbol{F_{rr} = C_{rr} M g \, Cos \, \Psi} \quad (3.2)$$

Where,

C_{rr} = Rolling resistance coefficient (dimensionless)

M = Gross mass of the vehicle (kg)

g = Gravitational acceleration (i.e., 9.81 ms^{-2})

Ψ = Grade angle (°)

The factor '$\mathrm{Cos}\,\Psi$' in Eq. (3.2) will only be taken into account, if there is an inclination on the road, as Ψ denotes the gradient of the road. $\mathrm{Cos}\,\Psi$ will be equal to 1, if the road is flat or has a gradient (=0°), since Cos 0°=1. Similar to this, if the road is slightly inclined, a very small value for Ψ can be considered and in this instance, the value of Cos Ψ will also be equal to 1.

This force is a self-generating force and is based on the GVW. According to Eq. (3.2), it is clear that the rolling resistance force will rise as the weight of the vehicle increases.

3.2.2 Aerodynamic Drag or Drag Force

Aerodynamic drag or drag force is the force that air resistance exerts against a moving vehicle. It is brought on by the shape of the vehicle and can be diminished by altering the shape to one that is more aerodynamic. A common man can feel this force by simply putting their hand outside the moving vehicle.

The equation for aerodynamic drag or drag force (F_{ad}) is:

$$\boldsymbol{F_{ad}} = \frac{1}{2}\rho A_f C_{ad}\boldsymbol{v^2} \tag{3.3}$$

Where,

ρ = Density of atmospheric air (i.e., 1.22 kgm^{-3} at 27°C)

A_f = Frontal area (m^2)

C_{ad} = Drag coefficient (dimensionless)

v = Resultant velocity of the vehicle and the wind (ms^{-1})

The most typical method of reducing aerodynamic drag or drag force is to utilize a spoiler, forming a low-pressure area on the back of the vehicle and lessening air resistance. According to Eq. (3.3), it is clear that the drag force is directly proportional to the square of velocity. If the velocity is doubled, then the drag force will increase by quadruple.

3.2.3 Hill Climbing Force or Gradient Force

Hill climbing force or gradient force, only comes into play when the path has an inclination, declination, or slope. From Fig. 3-3, it is clear that there are two components of vehicle weight, one parallel and one perpendicular to the inclined path, and their values are $Mg\,Sin\,\Psi$ and $Mg\,Cos\,\Psi$ respectively.

The equation for hill climbing force (F_{hc}) is:

$$\boldsymbol{F_{hc}} = M\boldsymbol{g}\,Sin\,\Psi \tag{3.4}$$

Where,

M = Gross mass of the vehicle (kg)

g = Gravitational acceleration (i.e., 9.81 ms^{-2})

Ψ = Grade angle (°)

Equation (3.4) will only be taken into account, if there is an inclination on the road, as Ψ denotes the gradient of the road. $Sin\,\Psi$ will be equal to 0, if the road is flat or has a gradient (=0°), since Sin 0°=0, which ultimately nullify the whole equation.

3.2.4 Linear Acceleration Force

Linear acceleration force is a force that is required to accelerate the vehicle.

The equation for linear acceleration force (F_{la}) is:

$$\boldsymbol{F_{la}} = M\boldsymbol{a} \tag{3.5}$$

Where,

M = Gross mass of the vehicle (kg)

a = Acceleration (ms^{-2})

The value of this force may be positive or negative depending on the velocity of the vehicle. As the vehicle decelerates, the value decreases and vice versa. Equation (3.5) shows that the linear acceleration force is directly proportional to the mass.

3.2.5 Rotational Acceleration Force

Rotational acceleration force is the force that is necessary to accelerate an object in a rotational motion. It is proportional to the mass of the object, its rotational velocity, and the rate of change of that velocity. This force is generated by a torque, which is the product of the moment of inertia and the angular acceleration.

The equation for rotational acceleration force ($F_{\omega a}$) is:

$$\boldsymbol{F_{\omega a}} = 0.1 \times \boldsymbol{F_{la}} \tag{3.6}$$

Where,

F_{la} = Linear acceleration force (N)

The extended form of Eq. (3.1) is given by combining Eq. (3.2), (3.3), (3.4), (3.5), and (3.6):

$$\boldsymbol{F_t} = C_{rr}\boldsymbol{Mg}\,Cos\,\Psi + \frac{1}{2}\rho A_f C_{ad}\boldsymbol{v^2} + \boldsymbol{Mg}\,Sin\,\Psi + \boldsymbol{Ma} + 0.1\boldsymbol{F_{la}} \tag{3.7}$$

The total tractive force required by a three-wheeler auto rickshaw in an IDC was calculated using the Eq. (3.7), based on selected specifications of a three-wheeler auto rickshaw (refer to Table 2-2). The various forces acting on an auto rickshaw in an IDC are depicted in Fig. 3-4.

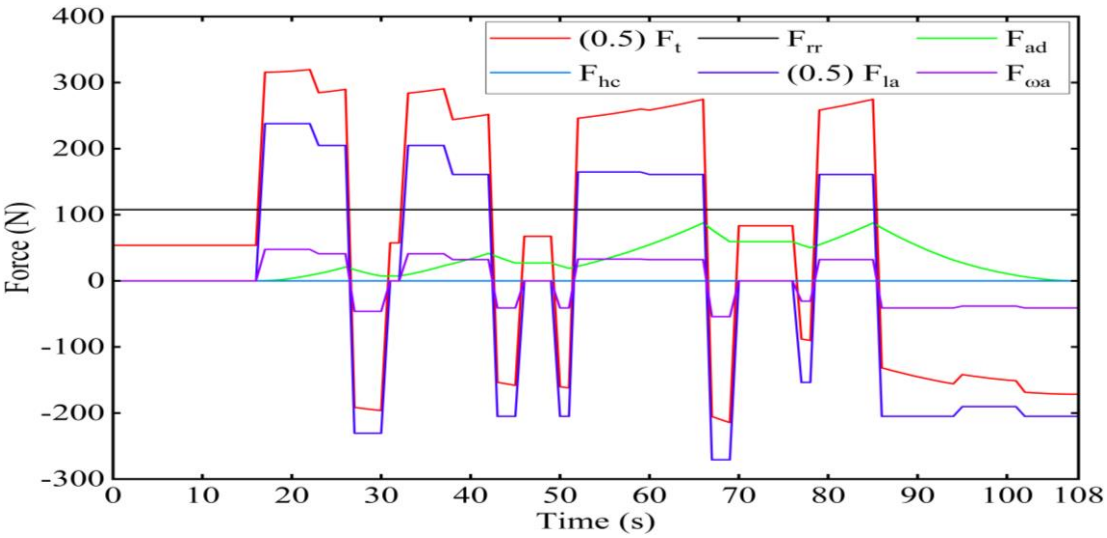

Fig. 3-4: Various forces acting on an auto rickshaw in an IDC

It can be ascertained that the acceleration force, F_{la}, is the major opposing force that the vehicle must overcome, becoming negative as the vehicle decelerates.

3.3 Estimation of Energy, Power and Torque

The selected specifications of an auto rickshaw used for road load modelling, is already outlined in Table 2-2. The Gross Vehicle Weight (GVW) is 732 kg with a Permanent-Magnet Synchronous Motor (PMSM) and a $LiFePO_4$, Lithium Ferro Phosphate (LFP), battery pack. A PMSM has been chosen over induction motor, Brushless DC (BLDC) motor and Switched Reluctance Motor (SRM) due to its relatively higher efficiency and torque. The efficiency coefficient of a PMSM ranges from 92% to 97%, an efficiency of 0.94 is assumed. $LiFePO_4$ battery pack is selected over Valve Sealed Lead Acid (VRLA) and nickel-metal hydride batteries for its longer life, zero maintenance, extremely safe, and most importantly, improved charging and discharging efficiency. Li-ion battery packs are increasingly popular and widely accepted in the automobile industry. Therefore, a Li-ion based pure electric auto rickshaw is considered for this study.

3.3.1 Power Demand

The tractive power, P_t, required at the wheels can be determined from the instantaneous tractive forces and the velocity of the vehicle, as depicted in Fig. 3-5, and is represented by the equation:

$$P_t = (\boldsymbol{F_t} \times R) \times \boldsymbol{v} \tag{3.8}$$

Where,

F_t = Tractive or traction force (N)

R = Regeneration efficiency (dimensionless)

υ = Resultant velocity of the vehicle and the wind (ms^{-1})

Regeneration efficiency is the fraction of energy recovered through regenerative braking system. It will only be taken into account, if F_t is negative in a particular operation in an IDC, else 1 is considered.

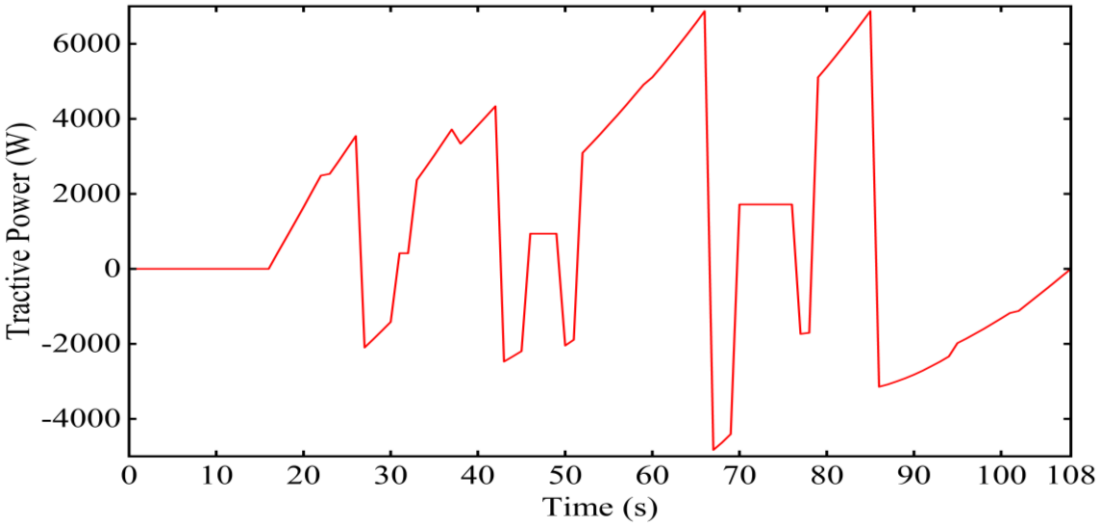

Fig. 3-5: Tractive power demand in an IDC

The motor power, P_m, required by the motor is derived from the tractive power, P_t, as depicted in Fig. 3-6, and is represented by the equation:

$$P_t \geq 0,\ P_m = \frac{P_t}{\eta_m}\ ;\ P_t < 0,\ P_m = P_t \times \eta_m \tag{3.9}$$

Where,

P_t = Tractive power (W)

η_m = Motor efficiency (dimensionless)

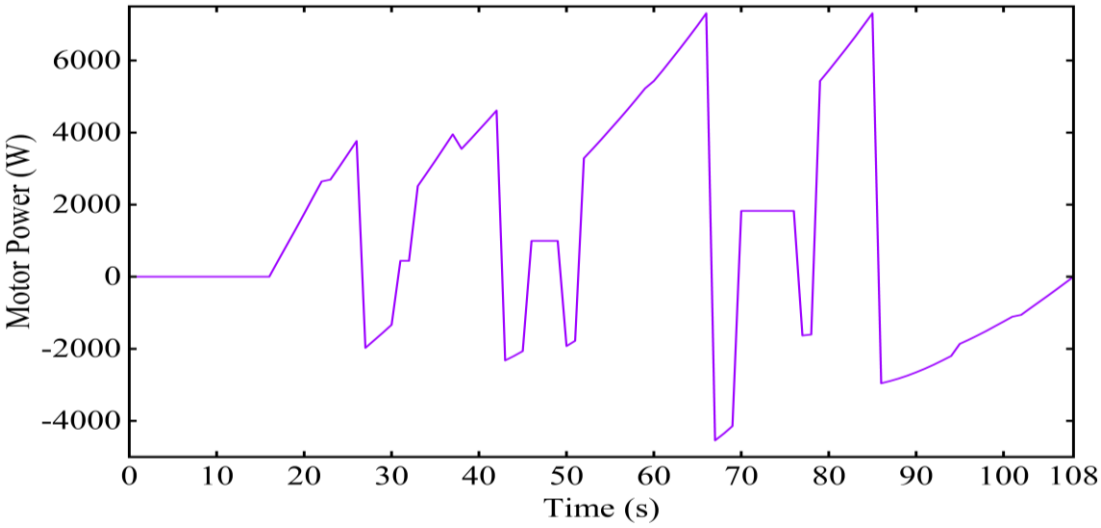

Fig. 3-6: Motor power demand in an IDC

The distribution of tractive and motor power in an IDC is depicted in Fig. 3-7.

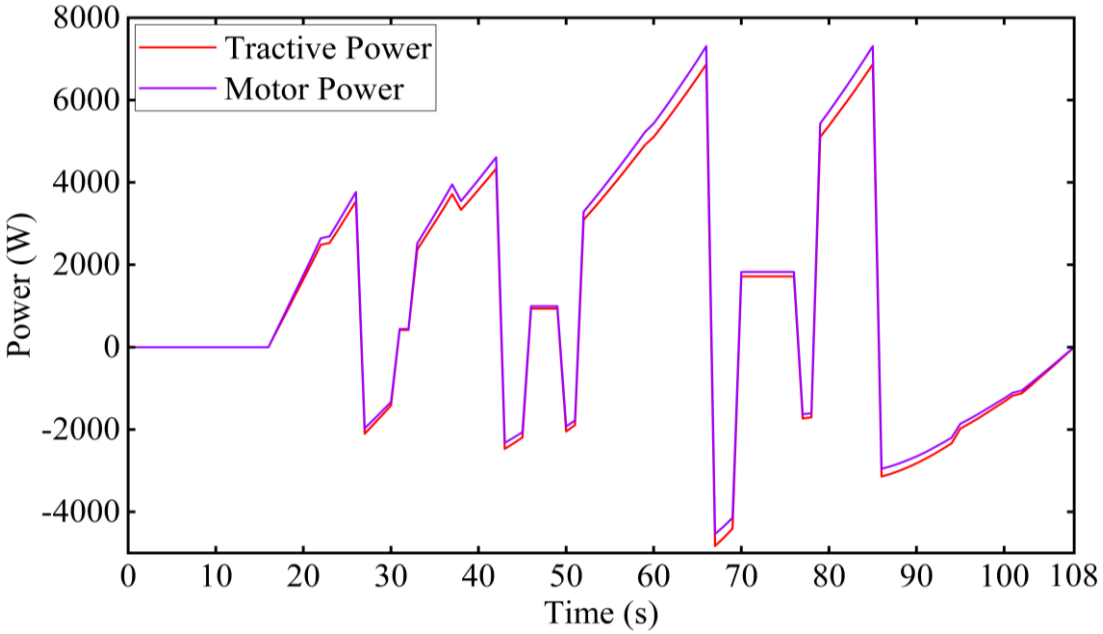

Fig. 3-7: Distribution of tractive and motor power in an IDC

3.3.2 Torque Demand

The tractive torque, T_t, distribution in an IDC is depicted in Fig. 3-8, and is represented by the equation:

$$\boldsymbol{T_t = F_t \times r_w} \tag{3.10}$$

Where,

F_t = Tractive force (N)

r_w = Radius of the wheel (m)

The motor torque, M_t, is represented by the equation:

$$\boldsymbol{M_t = \frac{G}{r_w} F_t} \tag{3.11}$$

Where,

G = Gear ratio (dimensionless)

r_w = Radius of the wheel (m)

F_t = Tractive force (N)

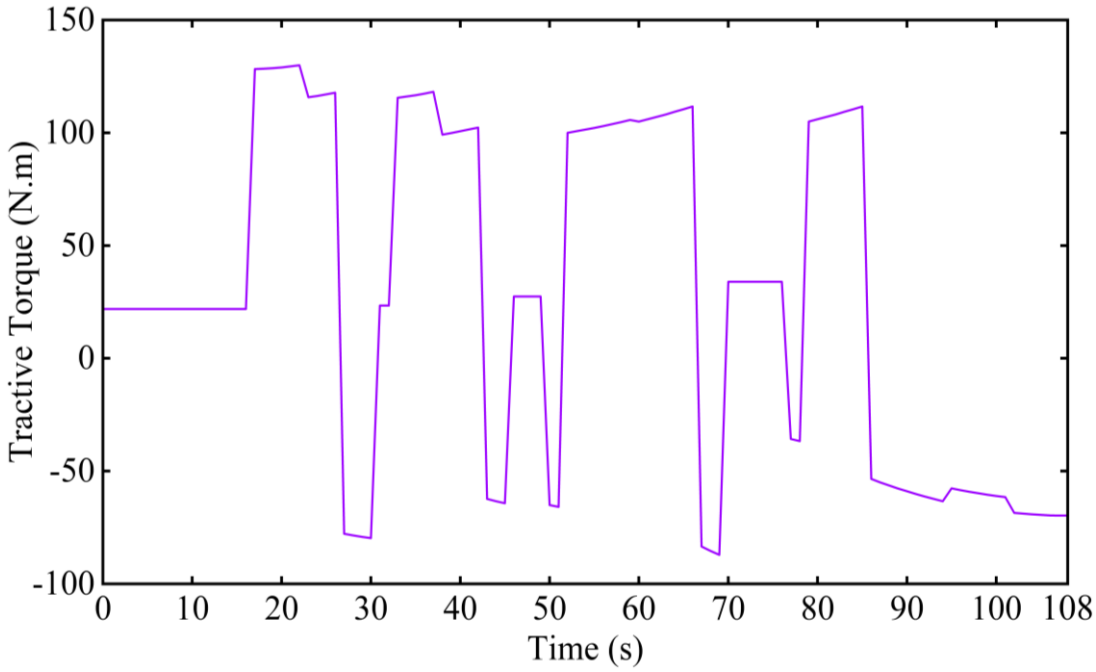

Fig. 3-8: Distribution of tractive torque in an IDC

Wheel Speed

Wheel speed, W_s, plays a major role in vehicle load modelling. It represents the rotational velocity of a vehicle's wheels and directly affects factors such as traction, stability and braking. Accurate wheel speed data is essential for evaluating vehicle dynamics, load distribution and overall performance. In load modelling, wheel speed help simulate real-world scenarios and predict how different loads affect a vehicle's motion and driveability, and is represented by the equation:

$$W_s = \frac{v}{2\pi r_w} \times \frac{60}{2\pi} \tag{3.12}$$

Where,

v = Resultant velocity of the vehicle and the wind (ms^{-1})

r_w = Radius of the wheel (m)

The change in wheel speed, with respect to the tractive torque, T_t, is depicted in Fig. 3-9.

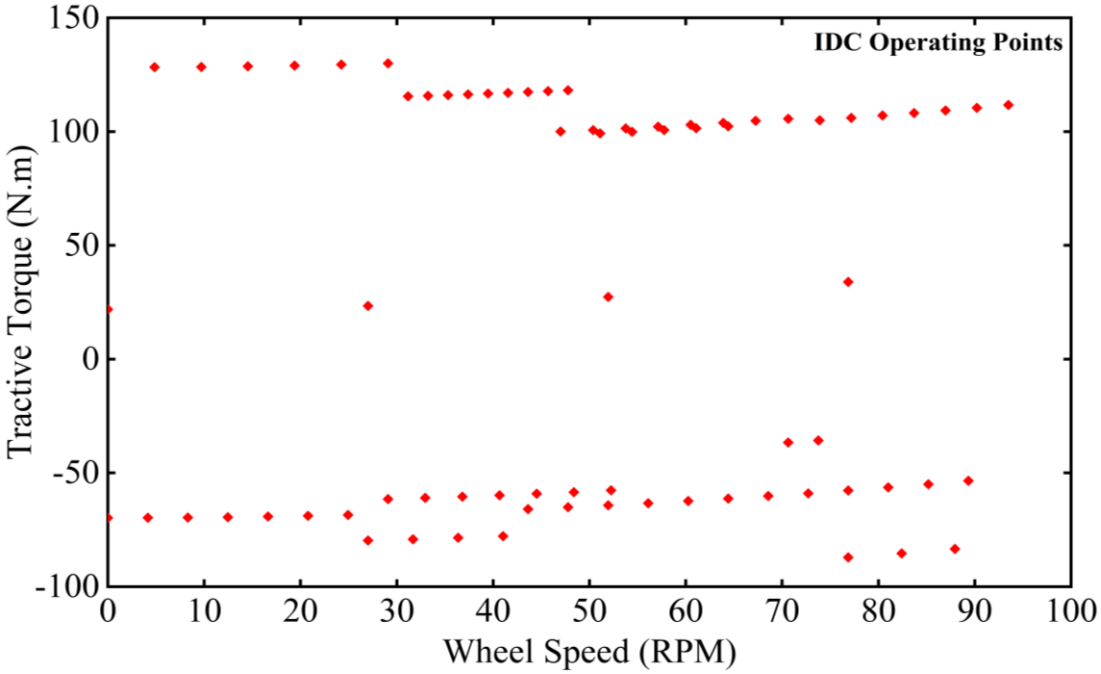

Fig. 3-9: Torque-speed operating points in an IDC

3.3.3 Energy Demand

The motor energy, E_m, demand at each operation in an IDC, is represented by the equation:

$$E_m = \int_{t1}^{t2} P_m \times dt \tag{3.13}$$

Where,

P_m = Motor power (W)

t = Time difference between each operation (s)

3.4 Regenerative Braking System

When a vehicle is in motion, it has kinetic energy and momentum. However, when the vehicle decelerates or brakes in traffic, this energy is wasted. According to the first law of thermodynamics, energy can neither be created nor be destroyed, it can only change from one form of energy to another. During braking, this kinetic energy is converted into frictional and thermal energy and is released into the environment. Using the regenerative braking concept, this energy can be reverted to the battery using the motor

[25, 26]. The powertrain of an EV automatically engages a regenerative braking system to make up for energy lost during deceleration and transfer the energy back to the motor, which now functions as a generator to charge the battery. This energy conversion is carried out by the motor of an EV.

In this work, four efficiencies of regenerative braking are considered, namely 0%, 40%, 50% and 100%. Regenerative braking efficiency at 0% means that no regenerative braking system is activated, while at 100% means that there is no energy loss, which is not possible because not all energy can be converted. Therefore, the regenerative braking efficiency of 40% and 50% seems more appropriate, as illustrated in Fig. 3-10.

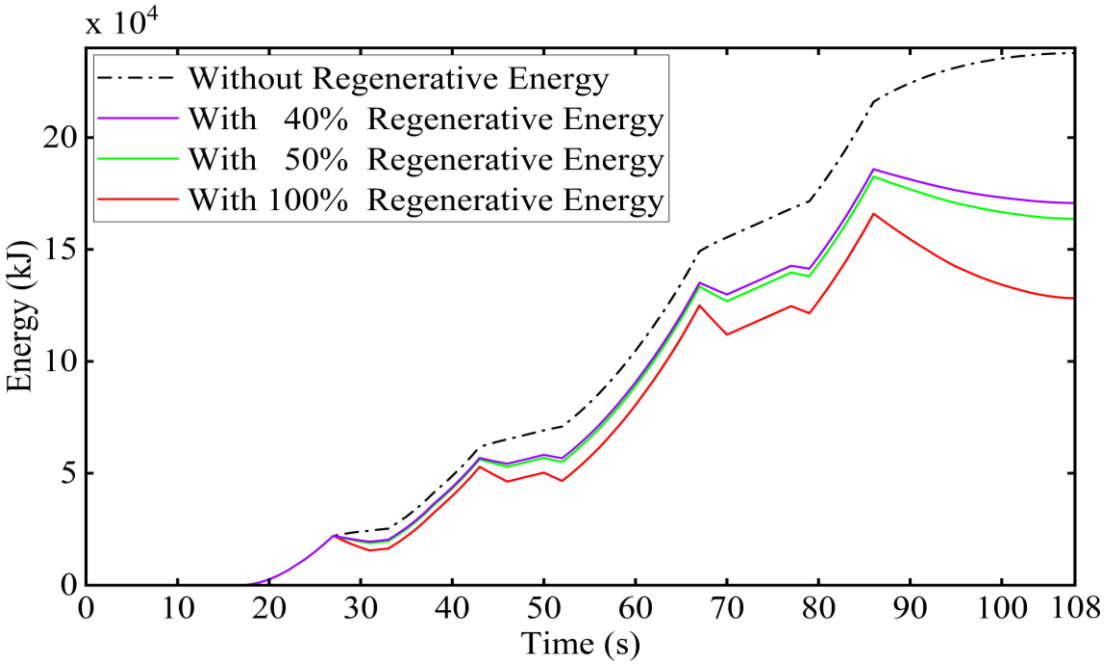

Fig. 3-10: Motor energy demand in an IDC

3.5 Determination of State of Charge

The State of Charge (SOC) is the ratio of the battery's remaining capacity to its total capacity, or the charge level of a battery related to its capacity. The SOC is 100% when the battery is completely charged and 0% when it is discharged. The SOC depends on many factors, such as temperature, charging and discharging current of the battery, also known as battery C-rate. C-rate is primarily the rate at which the battery is charged or discharged. 1C means the battery will be completely discharged in an hour and 2C

means the battery will be discharged in half an hour. There are several ways to find the SOC of a battery such as open voltage method, columb counting method, and the Kalman filter method [27]. Among all these methods of calculating SOC, the simple and generalized equation is given by:

$$SOC = 1 - \frac{Energy\ consumed\ in\ an\ operation}{Total\ Energy} \tag{3.14}$$

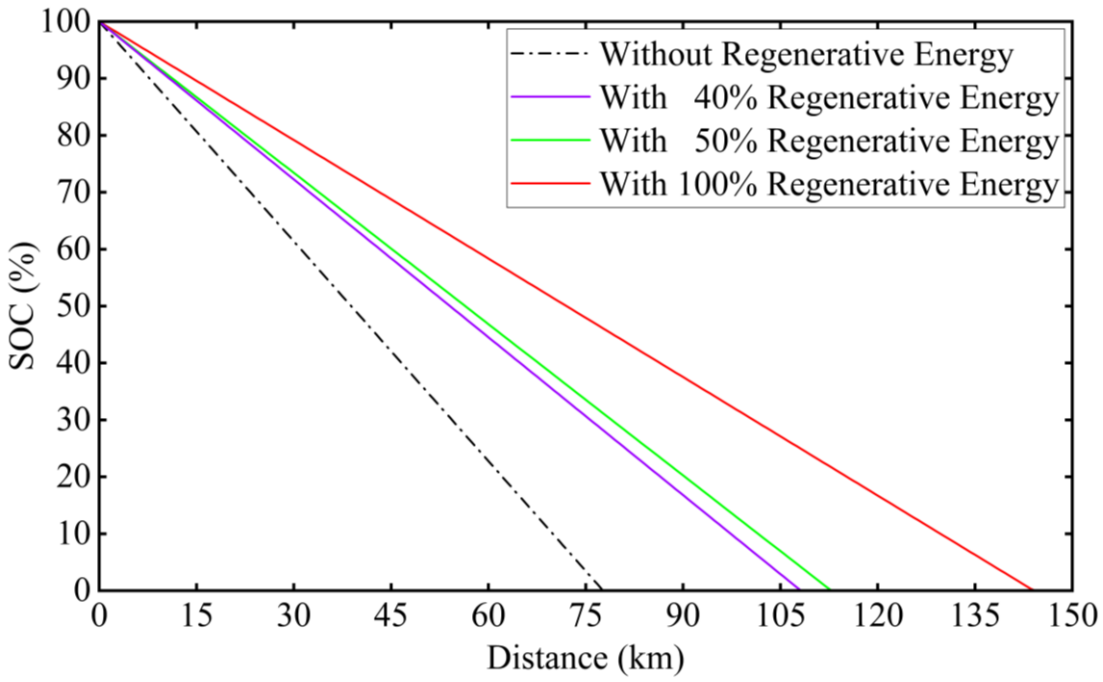

Fig. 3-11: Variation of SOC with distance

The graph above shows that with the selected vehicle, motor and battery specifications, the vehicle can travel up to 77.69 km on a single charge without regenerative braking. This distance can be extended to 108.216 km, 112.892 km and 144.288 km with a regeneration efficiency of 40%, 50% and 100% respectively.

Chapter 4

Results & Discussions

Range extension refers to the process of increasing the distance an Electric Vehicle (EV) can travel on a single battery charge. Increasing the range of Electric Vehicles (EVs) is essential to overcome the limitations of battery technology and alleviating range issues. Hybrid vehicles amalgamate an Internal Combustion Engine (ICE) with an electric motor and a battery. Range Extended Electric Vehicles (REEVs) have an electric motor powered by a battery and a standby ICE, such as a Micro Gas Turbines (MGT), generating electricity to extend the EV's range once the battery is depleted. However, for a pure EV, the range can only be increased by working more on battery technology, battery thermal management, improving the charging infrastructure, or via predictive driving assistance, optimizing driving routes and energy consumption based on real-time data. According to Para 3.1 (vi) of the guidelines and standards issued by the Ministry of Power, Government of India (refer to Table 1-1), it should be noted that a minimum of one charging station will be present within a radius of 25 km on either side of the highways. The selected three-wheeler auto rickshaw is a pure EV, following the iterated Indian Driving Cycle (IDC) to select and predict the performance of a powertrain system. An attempt is made to check the difference in range and energy consumption of the vehicle by capping the maximum velocity in an IDC, resulting in Modified Indian Driving Cycle (MIDC), for the last 25 km of the vehicle's ideal range. With the normal IDC (maximum velocity: 45 kmh^{-1}), 6 other Modified Indian Driving Cycles (MIDCs) were taken into consideration, whose maximum velocity is capped at 15 kmh^{-1}, 20 kmh^{-1}, 25 kmh^{-1}, 30 kmh^{-1}, 35 kmh^{-1} and 40 kmh^{-1} respectively, i.e., a difference of 5 kmh^{-1} in capping velocity between the different MIDCs. Using all the equations, formulations, and data from the previous chapter, the simulation begins with the range extension of a pure electric three-wheeler auto rickshaw.

IDC with a maximum velocity of 45 kmh^{-1} and 2 of the other 6 MIDCs with a capping velocity of 30 kmh^{-1} and 20 kmh^{-1} are shown in Fig. 4-1 and the data used to represent this figure is outlined in Table 4-1, 4-2, and 4-4.

Table 4-1: Velocity distribution in IDC and MIDCs

No. of operations	Velocity (kmh^{-1})							Duration of each operation (s)
	Capping Velocity (kmh^{-1})							
	IDC	MIDCs						
	45	40	35	30	25	20	15	
01	0	0	0	0	0	0	0	16
02	0-14	0-14	0-14	0-14	0-14	0-14	0-14	6
03	14-22	14-22	14-22	14-22	14-22	14-20	14-15	4
04	22-13	22-13	22-13	22-13	22-13	20-13	15-13	4
05	13	13	13	13	13	13	13	2
06	13-23	13-23	13-23	13-23	13-23	13-20	13-15	5
07	23-31	23-31	23-31	23-30	23-25	20	15	5
08	31-25	31-25	31-25	30-25	25	20	15	3
09	25	25	25	25	25	20	15	4
10	25-21	25-21	25-21	25-21	25-21	20	15	2
11	21-34	21-34	21-34	21-30	21-25	20	15	8
12	34-45	34-40	34-35	30	25	20	15	7
13	45-37	40-37	35	30	25	20	15	3
14	37	37	35	30	25	20	15	7
15	37-34	37-34	35-34	30	25	20	15	2
16	34-45	34-40	34-35	30	25	20	15	7
17	45-27	40-27	35-27	30-27	25	20	15	9
18	27-14	27-16	27-14	27-14	25-14	20-14	15-14	7
19	14-0	14-0	14-0	14-0	14-0	14-0	14-0	7
Cumulative Time (s)								**108**

Table 4-1 clearly shows that the number of steady state points, i.e., the points where velocity is constant or the initial and final velocity are equal, increases as the capping velocity in a cycle decreases. This symbolizes that if the vehicle is following MIDC with a lower capping velocity, it will have a greater number of steady state points in a cycle, and a greater number of steady state points means the vehicle is moving at a

constant velocity over a longer period of time in a cycle, resulting in zero acceleration at points where the vehicle is moving at constant velocity, as shown in Table 4-2.

Table 4-2: Acceleration distribution in IDC and MIDCs

No. of operations	Acceleration (ms^{-2})							Duration of each operation (s)
	Capping Velocity (kmh^{-1})							
	IDC	MIDCs						
	45	40	35	30	25	20	15	
01	0	0	0	0	0	0	0	16
02	0.65	0.65	0.65	0.65	0.65	0.65	0.65	6
03	0.56	0.56	0.56	0.56	0.56	0.42	0.07	4
04	-0.63	-0.63	-0.63	-0.63	-0.63	-0.49	-0.14	4
05	0	0	0	0	0	0	0	2
06	0.56	0.56	0.56	0.56	0.56	0.39	0.11	5
07	0.44	0.44	0.44	0.39	0.11	0	0	5
08	-0.56	-0.56	-0.56	-0.46	0	0	0	3
09	0	0	0	0	0	0	0	4
10	-0.56	-0.56	-0.56	-0.56	-0.56	0	0	2
11	0.45	0.45	0.45	0.31	0.14	0	0	8
12	0.44	0.24	0.04	0	0	0	0	7
13	-0.74	-0.28	0	0	0	0	0	3
14	0	0	0	0	0	0	0	7
15	-0.42	-0.42	-0.14	0	0	0	0	2
16	0.44	0.24	0.04	0	0	0	0	7
17	-0.56	-0.4	-0.25	-0.09	0	0	0	9
18	-0.52	-0.52	-0.52	-0.52	-0.44	-0.24	-0.04	7
19	-0.56	-0.56	-0.56	-0.56	-0.56	-0.56	-0.56	7
Cumulative Time (s)								**108**

Four different types of operating points in each driving cycle are idling, steady state points, accelerating points, and decelerating points. The duration of occurrence of each type of operating point varies between driving cycles. Table 4-3 shows the different operating point types and their durations of occurrence in IDC and MIDCs with different capping velocity, as well as the percentage contribution of each operating point type for different driving cycles.

Table 4-3: Operating points in IDC and MIDCs

Sl. No.	Particulars	Time (s)					Percentage (%)				
		Capping Velocity (kmh^{-1})					Capping Velocity (kmh^{-1})				
		IDC	MIDCs				IDC	MIDCs			
		45	35	30	25	20	45	35	30	25	20
1	Idling	16	16	16	16	16	14.81	14.81	14.81	14.81	14.81
2	Steady state points	13	16	32	44	59	12.04	14.81	29.63	40.74	54.63
3	Accelerating points	42	42	28	28	15	38.89	38.89	25.92	25.92	13.88
4	Decelerating points	37	34	32	20	18	34.26	31.48	29.63	18.52	16.66

IDC with a maximum velocity of 45 kmh^{-1} and MIDC with a capping velocity of 40 kmh^{-1} have the same duration of occurrence of each type of operating point. Similarly, the MIDCs with a capping velocity of 20 kmh^{-1} and 15 kmh^{-1} have the same duration of occurrence of each type of operating point. Therefore, the MIDCs with a capping velocity of 40 kmh^{-1} and 15 kmh^{-1} are not included in Table 4-3.

Distance distribution in IDC and 6 other MIDCs with different capping velocity is outlined in Table 4-4. It can be observed that the total distance travelled decreases as the capping velocity decreases.

Table 4-4: Distance distribution in IDC and MIDCs

No. of operations	Distance (m)							Duration of each operation (s)
	Capping Velocity (kmh^{-1})							
	IDC	MIDCs						
	45	40	35	30	25	20	15	
01	0	0	0	0	0	0	0	16
02	11.7	11.7	11.7	11.7	11.7	11.7	11.7	6
03	20.04	20.04	20.04	20.04	20.04	18.92	16.11	4
04	19.40	19.40	19.40	19.40	19.40	18.30	15.55	4
05	7.23	7.23	7.23	7.23	7.23	7.23	7.23	2
06	25.06	25.06	25.06	25.06	25.06	22.93	19.43	5
07	37.44	37.44	37.44	36.82	33.32	27.78	20.83	5
08	23.31	23.31	23.31	22.93	20.83	16.67	12.5	3
09	27.78	27.78	27.78	27.78	27.78	22.22	16.67	4
10	12.77	12.77	12.77	12.77	12.77	11.11	8.33	2
11	61.07	61.07	61.07	56.59	51.15	44.44	33.33	8
12	76.89	71.99	67.09	58.33	48.61	38.89	29.17	7
13	34.17	32.07	29.17	25	20.83	16.67	12.5	3
14	71.94	71.94	68.06	58.33	48.61	38.89	29.17	7
15	19.72	19.72	19.16	16.67	13.89	11.11	8.33	2
16	76.89	71.99	67.09	58.34	48.61	38.89	29.17	7
17	89.82	83.8	77.38	71.35	62.5	50	37.5	9
18	39.76	39.76	39.76	39.76	37.83	33.00	28.19	7
19	13.5	13.5	13.5	13.5	13.5	13.5	13.5	7
Total Distance (m)	**668.5**	**650.6**	**627**	**581.6**	**523.65**	**442.25**	**349.2**	
Cumulative Time (s)								**108**

Table 4-5 summarizes the important factors like total idling time, total time taken to travel the distance, total distance travelled by the vehicle, maximum velocity, average

velocity including stops, maximum acceleration, and maximum deceleration achieved by the vehicle in IDC and 6 other MIDCs with different capping velocity.

Table 4-5: Summary of IDC and MIDCs

	IDC	MIDCs					
Capping Velocity (kmh^{-1})	**45**	**40**	**35**	**30**	**25**	**20**	**15**
Idling time (s) in a cycle	16	16	16	16	16	16	16
Total time (s) taken in a cycle	108	108	108	108	108	108	108
Total distance (km) travelled in a cycle	0.668	0.650	0.627	0.581	0.523	0.442	0.349
Maximum velocity (kmh^{-1})	45	40	35	30	25	20	15
Average velocity incl. stops (kmh^{-1})	22.29	21.69	20.91	19.39	17.46	14.74	11.64
Maximum acceleration (ms^{-2})	0.65	0.65	0.65	0.65	0.65	0.65	0.65
Maximum deceleration (ms^{-2})	0.74	0.63	0.63	0.63	0.63	0.56	0.56

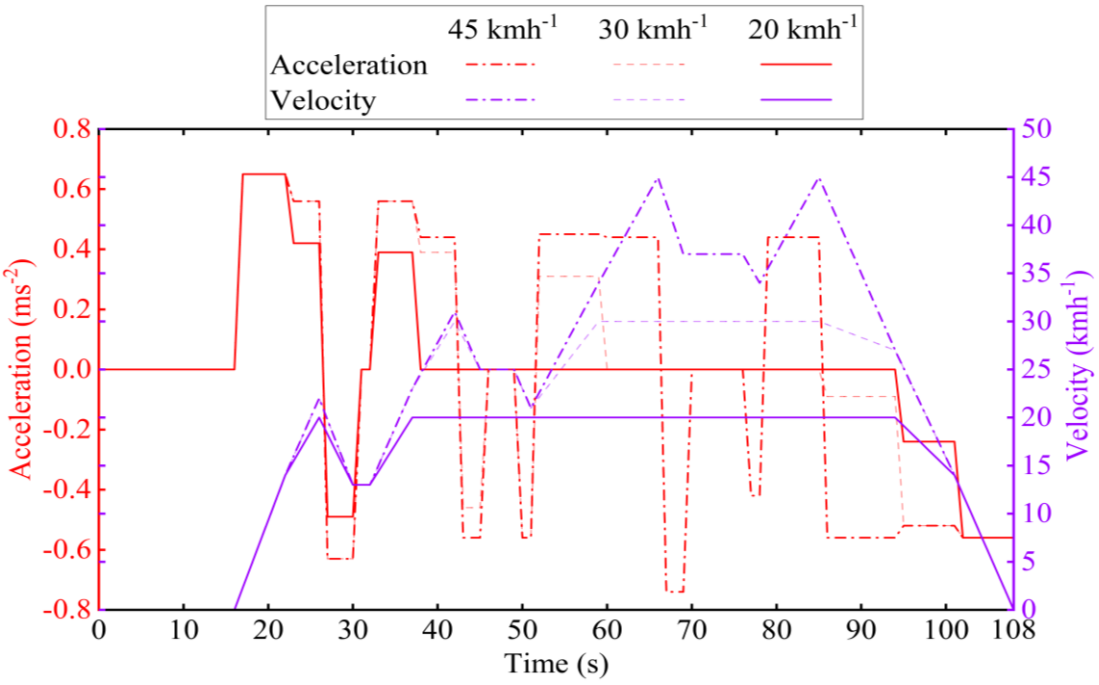

Fig. 4-1: MIDCs in contrast to IDC (capping velocity: 30 and 20 kmh^{-1})

The total tractive force required for a three-wheeler auto rickshaw following the MIDC with a capping velocity of 20 kmh^{-1} together with the various forces acting on it is calculated using Eq. (3.1 – 3.7), stationed on the selected specifications of an auto rickshaw (refer to Table 2-2). The various forces acting on a three-wheeler auto rickshaw in MIDC with a capping velocity of 20 kmh^{-1} are depicted in Fig. 4-2.

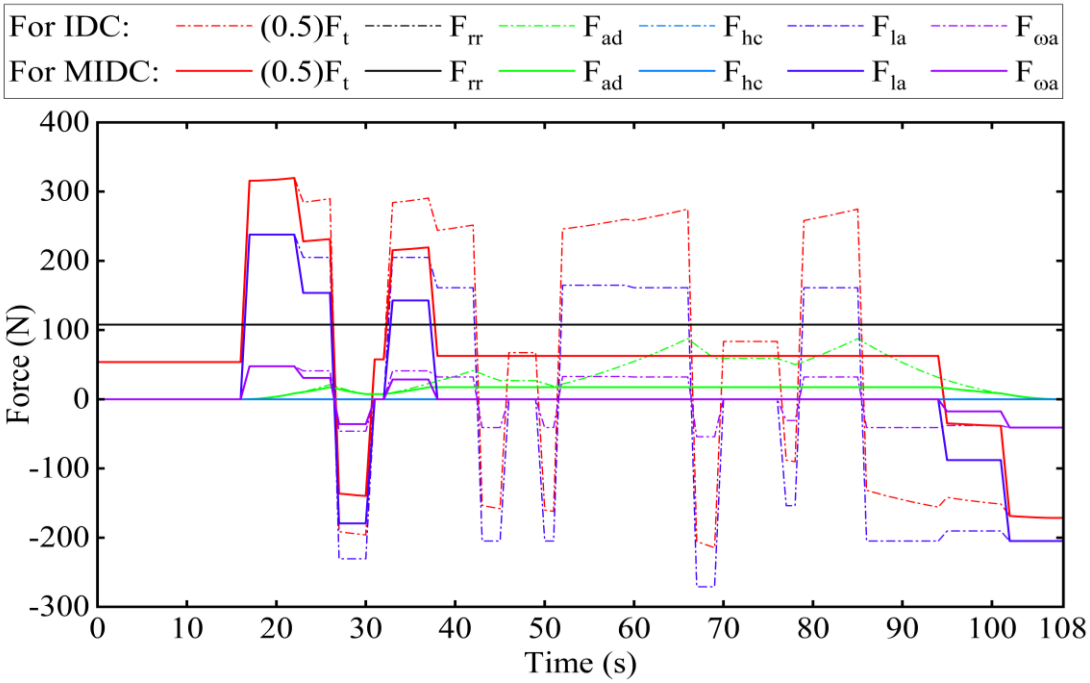

Fig. 4-2: Various forces acting on an auto rickshaw in MIDC

Figure 4-2 shows that the values of the various forces acting on an auto rickshaw in MIDC with a capping velocity of 20 kmh^{-1} are significantly lower compared to IDC, which will result in less power demand.

4.1 Determination of Energy, Power and Torque Demand

The tractive power, P_t, required at the wheels can be determined from the instantaneous tractive forces and the velocity of the vehicle, and is calculated using Eq. (3.8), as depicted in Fig. 4-3.

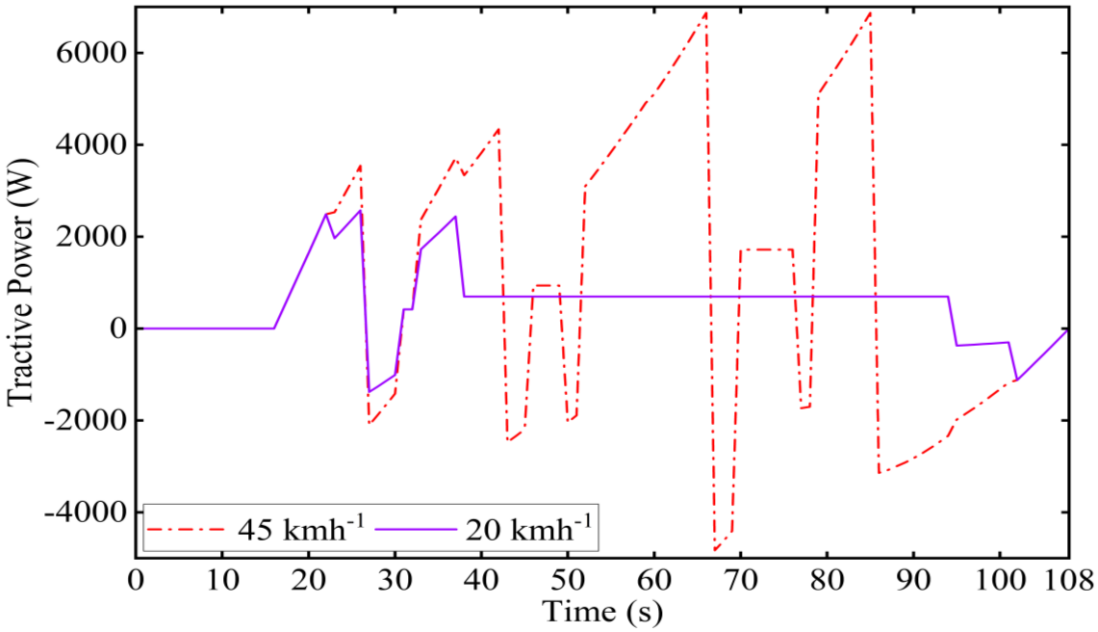

Fig. 4-3: Tractive power demand

The motor power, P_m, required by the motor is derived from the tractive power, P_t, and is calculated using Eq. (3.9), as depicted in Fig. 4-4.

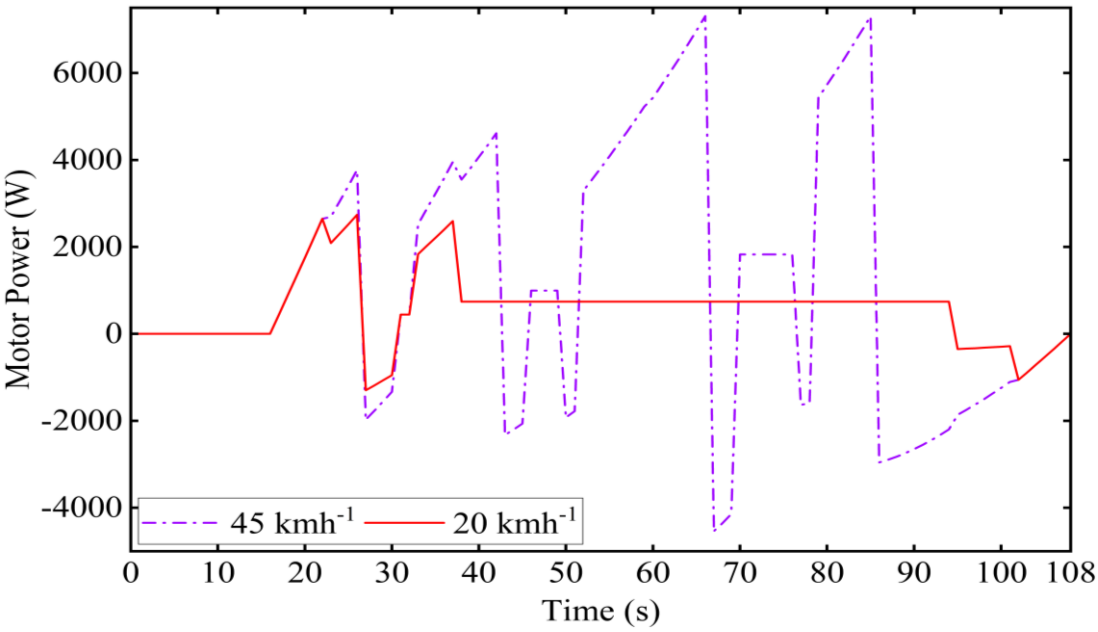

Fig. 4-4: Motor power demand

The distribution of tractive and motor power in IDC and MIDC with a capping velocity of 20 kmh^{-1} is depicted in Fig. 4-5.

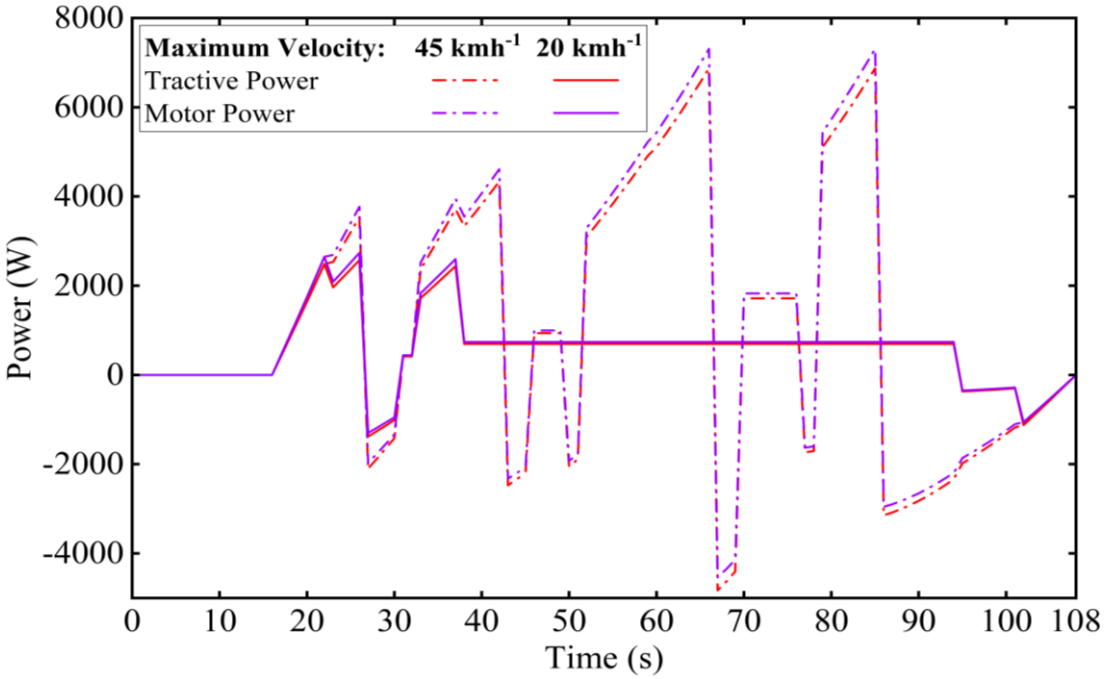

Fig. 4-5: Distribution of tractive and motor power

Figure 4-5 shows that the tractive and motor power demand for MIDC with a capping velocity of 20 kmh^{-1} are much lower than that for IDC, and both power demands remained constant for more than 50 s in a driving cycle of 108 s.

Distribution of tractive torque, T_t, is calculated using Eq. (3.10), and is depicted in Fig. 4-6. Figure 4-6 shows that initially the tractive torque demand was almost the same for both IDC and MIDC with a capping velocity of 20 kmh^{-1}, but later the torque demand for MIDC with a capping velocity of 20 kmh^{-1} was much less than the corresponding IDC.

The change in wheel speed, calculated using Eq. (3.12), with respect to the tractive torque, T_t, is depicted in Fig. 4-7 and it is to be noted that the wheel speed for MIDC with a capping velocity of 20 kmh^{-1} was much lower than that for IDC.

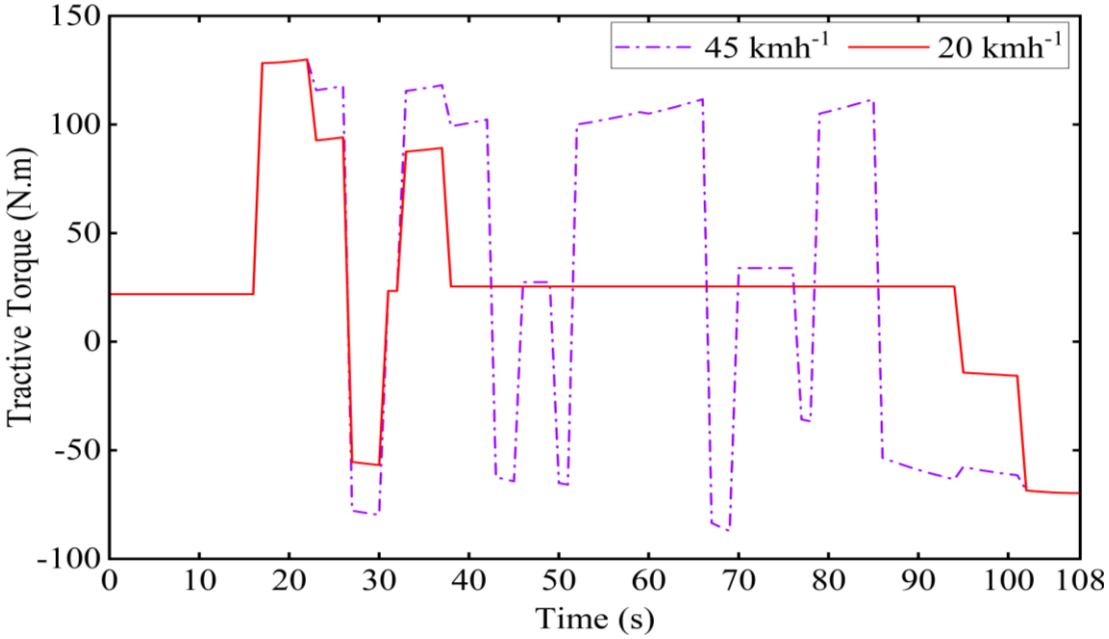

Fig. 4-6: Distribution of tractive torque

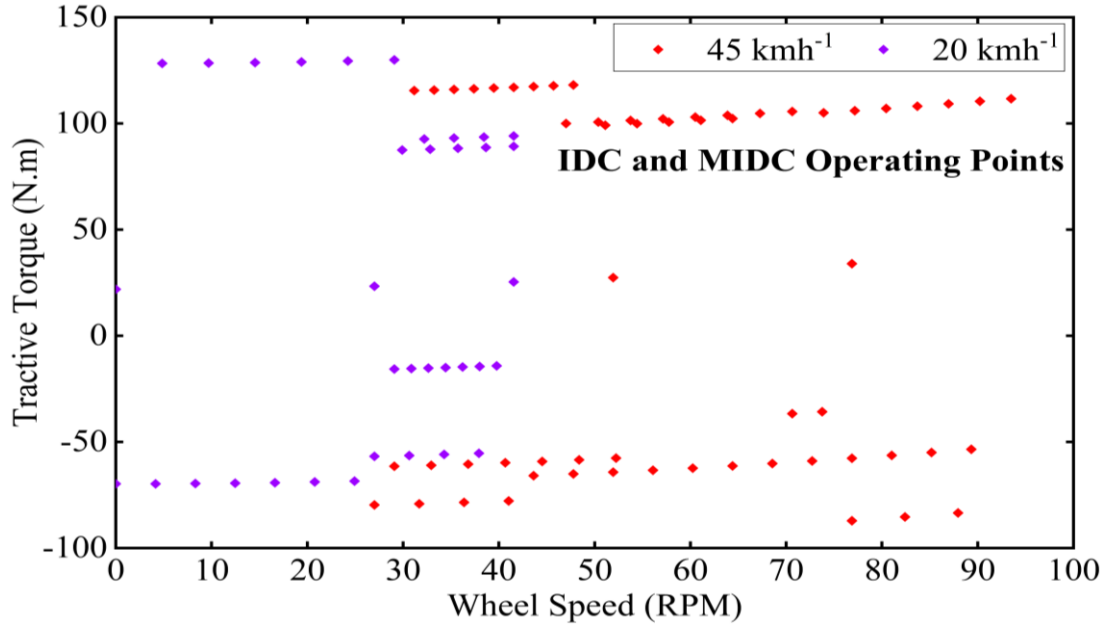

Fig. 4-7: Torque-speed operating points

The motor energy, E_m, demand with different regeneration efficiencies in each operation of IDC and MIDC with a capping velocity of 20 kmh^{-1} is calculated using Eq. (3.13), and is depicted in Fig. 4-8.

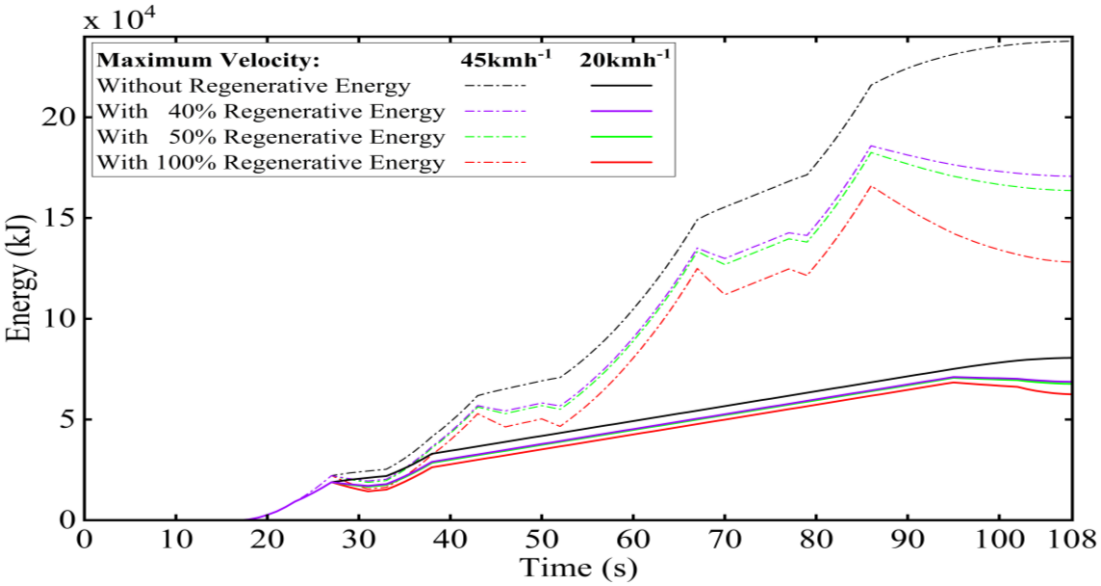

Fig. 4-8: Motor energy demand with different regeneration efficiencies

Figure 4-8 shows that the energy demand is quite linear and much lower for MIDC with a capping velocity of 20 kmh^{-1} than for IDC and lower energy demand means that energy consumption will be lower.

4.2 Determination of State of Charge (SOC)

The State of Charge (SOC) is calculated using Eq. (3.14), and the graph between SOC and distance is shown in Fig. 4-9.

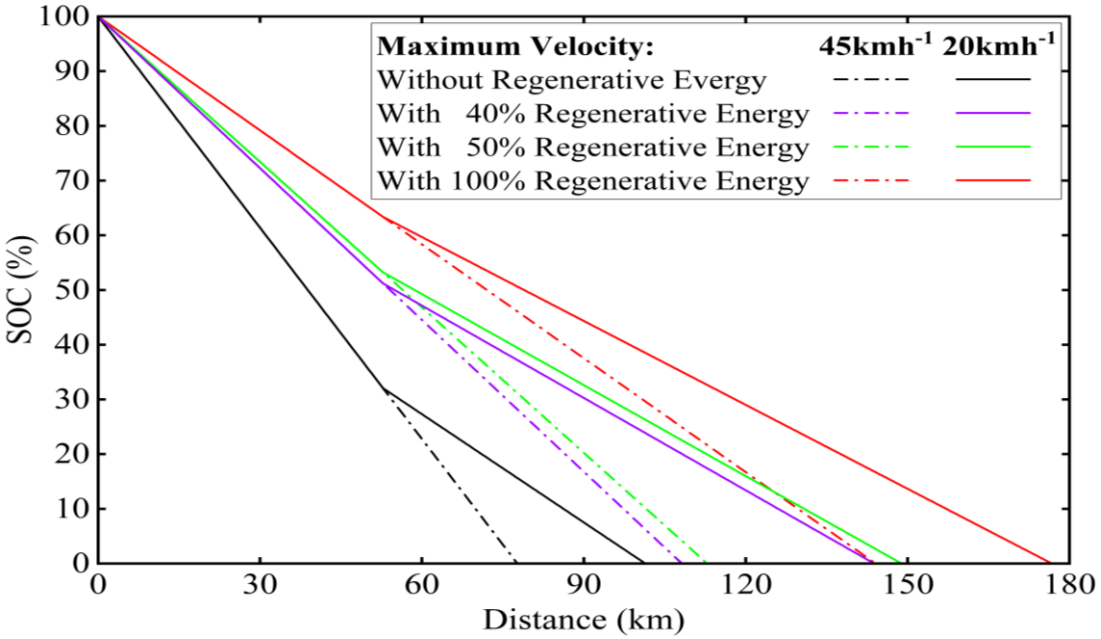

Fig. 4-9: Variation of SOC with distance

It can be seen from the figure above that the SOC decreases at a constant rate, deviating from a point of 52.69 km on the x-axis, which means that the vehicle has started to follow the MIDC with a capping velocity of 20 kmh^{-1} from this point, further extending the range. However, the level of SOC drop is not the same for different regenerative braking efficiencies.

With the selected vehicle specifications, the initial range of a three-wheeler auto rickshaw was found to be 77.69 km with regenerative braking efficiency of 0% or without regeneration, 108.22 km with regenerative braking efficiency of 40%, and 112.89 km with regenerative braking efficiency of 50%. This initial range difference is only due to the different regenerative braking efficiencies. An overall increment in range of 39.29% and 45.30% can be achieved only by using regenerative braking efficiency of 40% and 50%, respectively. The vehicle initially follows IDC and before 25 km from the initial range with regenerative braking efficiency of 0% or without regeneration, i.e., from 52.69 km, the vehicle starts following MIDC with a capping velocity of 20 kmh^{-1}, extending the range to 101.83 km. Similarly, this range is further extended to 143.82 km and 149.13 km using regenerative braking efficiency of 40% and 50%, respectively.

The overall energy consumption, the total amount of energy that can be conserved, and the range that can be extended using the amount of energy saved by using different regenerative braking efficiencies and MIDCs with different capping velocity for the last 25 km of the initial range are outlined in Table 4-6, Table 4-7 and Table 4-8.

Table 4-6: Overall energy consumption

	Energy Consumption (kWh)						
	IDC	**IDC + MIDC (last 25 km of initial range)**					
	Max. Velocity (kmh^{-1})	**Capping Velocity (kmh^{-1})**					
	45	**40**	**35**	**30**	**25**	**20**	**15**
With 0% Regenerative Energy	7.68	7.37	7.10	6.92	6.70	6.47	6.28
With 40% Regenerative Energy	5.52	5.31	5.16	5.08	4.98	4.82	4.70
With 50% Regenerative Energy	5.29	5.10	4.97	4.89	4.80	4.65	4.54

Table 4-7: Total energy conserved

	Energy Conserved (kWh)						
	IDC	**IDC + MIDC (last 25 km of initial range)**					
	Max. Velocity (kmh^{-1})	**Capping Velocity (kmh^{-1})**					
	45	**40**	**35**	**30**	**25**	**20**	**15**
With 0% Regenerative Energy	0	0.31	0.58	0.76	0.98	1.21	1.4
With 40% Regenerative Energy	2.16	2.37	2.52	2.6	2.7	2.86	2.98
With 50% Regenerative Energy	2.39	2.58	2.71	2.79	2.88	3.03	3.14

Table 4-8: Effective ranges after extension

	Range Extension (km)						
	IDC	**IDC + MIDC (last 25 km of initial range)**					
	Max. Velocity (kmh^{-1})	**Capping Velocity (kmh^{-1})**					
	45	**40**	**35**	**30**	**25**	**20**	**15**
With 0% Regenerative Energy	77.69 (0)	81.42 (3.73)	85.38 (7.69)	88.86 (11.17)	94.17 (16.48)	101.83 (24.14)	110.36 (32.67)
With 40% Regenerative Energy	108.22 (30.53)	115.92 (38.23)	122.37 (44.68)	126.10 (48.41)	132.42 (54.73)	143.82 (66.13)	155.73 (78.04)
With 50% Regenerative Energy	112.89 (35.2)	120.48 (42.79)	126.76 (49.07)	131.34 (53.65)	137.66 (59.97)	149.13 (71.44)	160.61 (82.92)

It can be predicted from the tables above that if the vehicle uses a regenerative braking system and MIDC with a capping velocity, also coined as an energy saving mode, for the last 25 km of its range, the overall range will increase as the capping velocity of the MIDC decreases.

Chapter 5

Conclusion & Scope for Future Work

5.1 Conclusion

In this work, the range extension of a pure electric three-wheeler auto rickshaw is performed without a Range Extender (RE). A parametric study was conducted to appraise the impact of the regenerative braking system and the Modified Indian Driving Cycle (MIDC) on the driving range of an auto rickshaw under Indian road conditions.

The maximum velocity in MIDC is capped at different velocities in order to check its impact on the overall range of the vehicle. It has been observed that vehicle range increases significantly as capping velocity decreases, meaning that MIDC with a capping velocity of 20 kmh^{-1} will provide better range than MIDC with a capping velocity of 40 kmh^{-1}. However, as the capping velocity decreases, the time it takes to cover the distance increases. The combination of an increase in regenerative energy efficiency and a decrease in the capping velocity will help conserve energy, which certainly contributes to increase the range of the vehicle.

The range of the vehicle calculated with the selected vehicle specifications was initially 77.69 km. The range was subsequently increased by 39.29% and 45.30%, extending to 108.22 km and 112.89 km using 40% and 50% of the energy gained through regenerative energy, respectively. From the point of 52.69 km, MIDC with a capping velocity of 20 kmh^{-1} was followed, designated as ‘Energy Saving Mode’. After complying with MIDC, the total range was increased by 85.12% and 91.95%, extending the overall range to 143.82 km and 149.13 km, respectively. The combination of regeneration energy and MIDC seems eminent for extending the range of the vehicle.

5.2 Future Scope

- A Li-ion battery pack with lower capacity could be designed if the conserved energy is not leveraged in extending the range, making the vehicle lighter.
- A Range Extender (RE) could be introduced to further extend range by charging the battery on the go while driving.
- A real-time range monitoring application could be developed to continuously monitor the battery status.

References

[1] Singh, R., Malik, A., “Auto industry pins hope on consumption-led demand in Budget for revival of growth,” in The Economic Times, Jan 2022, https://economictimes.indiatimes.com/small-biz/sme-sector/auto-industry-pins-hope-on-consumption-led-demand-in-budget-for-revival-of-growth/articleshow/89235273.cms. Accessed 19 June 2023

[2] Ministry of Power, Government of India, “Charging Infrastructure for Electric Vehicles (EV): Guidelines and Standards,” No. 12/2/2018-EV (Comp No. 244347), pp.4-9, Jan 2022, https://powermin.gov.in/sites/default/files/webform/notices/Final_Consolidated_EVCI_Guidelines_January_2022_with_ANNEXURES.pdf. Accessed 19 June 2023

[3] NITI Aayog, Government of India, http://www.niti.gov.in/. Accessed 19 June 2023

[4] Ribau, J., Silva, C., Brito, F. P., & Martins, J. (2012). Analysis of four-stroke, Wankel, and microturbine based range extenders for electric vehicles. Energy Conversion and Management, 58, 120-133.

[5] Bobba, P. B., & Rajagopal, K. R. (2012, December). Modelling and analysis of hybrid energy storage systems used in electric vehicles. In 2012 IEEE International Conference on Power Electronics, Drives and Energy Systems (PEDES) (pp. 1-6). IEEE.

[6] Marker, S., Rippel, B., Waldowski, P., Schulz, A., & Schindler, V. (2013). Battery Electric Vehicle (BEV) or Range Extended Electric Vehicle (REEV)? — Deciding Between Different Alternative Drives Based on Measured Individual Operational Profiles. Oil & Gas Science and Technology–Revue d’IFP Energies nouvelles, 68(1), 65-77.

[7] Mishra, P., Saha, S., & Ikkurti, H. P. (2013, April). Selection of propulsion motor and suitable gear ratio for driving electric vehicle on Indian city roads. In 2013 International Conference on Energy Efficient Technologies for Sustainability (pp. 692-698). IEEE.

[8] Sreejith, R., & Rajagopal, K. R. (2016, July). An insight into motor and battery selections for three-wheeler electric vehicle. In 2016 IEEE 1st International Conference on Power Electronics, Intelligent Control and Energy Systems (ICPEICES) (pp. 1-6). IEEE.

[9] Xian, T. F., Soon, C. M., Rajoo, S., & Romagnoli, A. (2016, October). A parametric study: The impact of components sizing on range extended electric vehicle's driving range. In 2016 Asian Conference on Energy, Power and Transportation Electrification (ACEPT) (pp. 1-6). IEEE.

[10] Vidhya, S. D., & Balaji, M. (2019). Modelling, design and control of a light electric vehicle with hybrid energy storage system for Indian driving cycle. Measurement and control, 52(9-10), 1420-1433.

[11] Tran, M. K., Bhatti, A., Vrolyk, R., Wong, D., Panchal, S., Fowler, M., & Fraser, R. (2021). A review of range extenders in battery electric vehicles: Current progress and future perspectives. World Electric Vehicle Journal, 12(2), 54.

[12] Navaneeth, M., Jithin, J., Ali, M. J., & Swathi, P. V. (2021, June). Improved E-bike charger suitable for advanced charging algorithms. In 2021 International Conference on Communication, Control and Information Sciences (ICCISc) (Vol. 1, pp. 1-5). IEEE.

[13] Mohammed, A. S., Salau, A. O., Sigweni, B., & Zungeru, A. M. (2023). Conversion and Performance Evaluation of Petrol Engine to Electric Powered Three-Wheeler Vehicle with an Onboard Solar Charging System. Energy Conversion and Management: X, 100427.

[14] Bajaj RE E-TEC 9.0 – Specifications, (2022), Bajaj Auto Ltd., https://www.bajajauto.com/three-wheelers/ev-re. Accessed 19 June 2023

[15] Circular on approval of the competent authority (DC/OPS/Tpt/598/2016/2570), (2020), Transport Department, Government of NCT of Delhi, https://it.delhigovt.nic.in/writereaddata/Cir2020751974.pdf. Accessed 19 June 2023

[16] Bajaj RE - Full Specifications, Bajaj Auto Ltd., https://www.bajajauto.com/three-wheelers/re/specifications. Accessed 19 June 2023

[17] Data Sheet for SIMOTICS S-1FK7, Siemens, https://mall.industry.siemens.com/mall/en/it/Catalog/Product/1FK7042-2AF71-1CH0. Accessed 19 June 2023

[18] Technical specifications of 8.9 kWh LiFePO4 High Performance Cells, Vision Mechatronics, https://vmechatronics.com/lithium-ion-battery-lirackeco. Accessed 19 June 2023

[19] Automotive Industry Standard: Test Method, Testing Equipment and Related Procedures for Type Approval and Conformity of Production (COP) Testing of L5 Category Vehicles as per CMV Rules 115, 116 and 126 (AIS-137 (Part 2)), Ministry of Road Transport & Highways, Government of India; The Automotive Research Association of India, https://morth.nic.in/sites/default/files/ASI/524201950214PMAIS_137_Part_2_F.pdf. Accessed 19 June 2023

[20] Singh, S. K., Sikri, G., & Garg, M. (2008). Body Mass Index and Obesity: Tailoring "cut-off" for an Asian Indian Male Population. Medical Journal, Armed Forces India, 64(4), 351. https://doi.org/10.1016/s0377-1237(08)80019-6.

[21] Automotive Research Association of India (ARAI), Document on test method, testing equipment and related procedures for testing type approval and conformity of production (COP) of vehicles for emission as per CMV rules 115, 116 and 126, https://www.araiindia.com/CMVR_TAP%20Documents/Part-14/Part-14_Chapter03.pdf. Accessed 19 June 2023

[22] Mallouh, M. A., Denman, B., Surgenor, B., & Peppley, B. (2010). A study of fuel cell hybrid auto rickshaws using realistic urban drive cycles. JJMIE, 4(1), 225-229.

[23] Shah, V., Pritesh, P., & Sagar, P. (2011). Measurement of real time drive cycle for Indian roads and estimation of component sizing for HEV using LABVIEW. International Journal of Electrical and Computer Engineering, 5(10), 1112-1120.

[24] Breakdown of the operating cycle used for the test as per CMV rule 115 (3) – Annexure II, https://www.roadsafetynetwork.in/wp-content/uploads/2019/01/cmvr-1989-annotated.pdf. Accessed 19 June 2023

[25] Cody, J., Göl, Ö., Nedic, Z., Nafalski, A., & Mohtar, A. (2009). Regenerative braking in an electric vehicle. Maszyny Elektryczne: zeszyty problemowe, (81), 113-118.

[26] GÜNEY, B., & KILIÇ, H. Research on Regenerative Braking Systems: A.

[27] Murnane, M., & Ghazel, A. (2017). A closer look at state of charge (SOC) and state of health (SOH) estimation techniques for batteries. Analog devices, 2, 426-436.